

Lawrence Berkeley National Laboratory

Joint Genome Institute

Title

Mixotrophic Iron-Oxidizing Thiomonas Isolates from an Acid Mine Drainage-Affected Creek.

Permalink

<https://escholarship.org/uc/item/47j1p3kh>

Journal

Applied and Environmental Microbiology, 86(24)

ISSN

0099-2240

Authors

Akob, Denise M
Hallenbeck, Michelle
Beulig, Felix
et al.

Publication Date

2020-11-24

DOI

10.1128/aem.01424-20

Peer reviewed



Mixotrophic Iron-Oxidizing *Thiomonas* Isolates from an Acid Mine Drainage-Affected Creek

 Denise M. Akob,^a Michelle Hallenbeck,^{b,h} Felix Beulig,^{c,*} Maria Fabisch,^c Kirsten Küsel,^c  Jessica L. Keffer,^{g,h}
 Tanja Woyke,^d Nicole Shapiro,^d Alla Lapidus,^{d,e}  Hans-Peter Klenk,^f  Clara S. Chan^{b,g,h}

^aU.S. Geological Survey, Reston, Virginia, USA

^bDepartment of Biological Sciences, University of Delaware, Newark, Delaware, USA

^cInstitute of Biodiversity, Friedrich Schiller University Jena, Jena, Germany

^dJoint Genome Institute, U.S. Department of Energy, Berkeley, California, USA

^eCenter for Algorithmic Biotechnology, St. Petersburg State University, St. Petersburg, Russia

^fSchool of Natural and Environmental Sciences, Newcastle University, Newcastle upon Tyne, United Kingdom

^gDepartment of Earth Sciences, University of Delaware, Newark, Delaware, USA

^hDelaware Biotechnology Institute, Newark, Delaware, USA

Denise M. Akob and Michelle Hallenbeck contributed equally to this work. Author order was determined via discussion and agreement between D.M.A. and M.H., based on the fact that D.M.A. took the lead in bringing all of the experiments and writing together, while M.H. took the lead on genome analysis.

ABSTRACT Natural attenuation of heavy metals occurs via coupled microbial iron cycling and metal precipitation in creeks impacted by acid mine drainage (AMD). Here, we describe the isolation, characterization, and genomic sequencing of two iron-oxidizing bacteria (FeOB) species: *Thiomonas ferrovorans* FB-6 and *Thiomonas metallidurans* FB-Cd, isolated from slightly acidic (pH 6.3), Fe-rich, AMD-impacted creek sediments. These strains precipitated amorphous iron oxides, lepidocrocite, goethite, and magnetite or maghemite and grew at a pH optimum of 5.5. While *Thiomonas* spp. are known as mixotrophic sulfur oxidizers and As oxidizers, the FB strains oxidized Fe, which suggests they can efficiently remove Fe and other metals via coprecipitation. Previous evidence for *Thiomonas* sp. Fe oxidation is largely ambiguous, possibly because of difficulty demonstrating Fe oxidation in heterotrophic/mixotrophic organisms. Therefore, we also conducted a genomic analysis to identify genetic mechanisms of Fe oxidation, other metal transformations, and additional adaptations, comparing the two FB strain genomes with 12 other *Thiomonas* genomes. The FB strains fall within a relatively novel group of *Thiomonas* strains that includes another strain (b6) with solid evidence of Fe oxidation. Most *Thiomonas* isolates, including the FB strains, have the putative iron oxidation gene *cyc2*, but only the two FB strains possess the putative Fe oxidase genes *mtaAB*. The two FB strain genomes contain the highest numbers of strain-specific gene clusters, greatly increasing the known *Thiomonas* genetic potential. Our results revealed that the FB strains are two distinct novel species of *Thiomonas* with the genetic potential for bioremediation of AMD via iron oxidation.

IMPORTANCE As AMD moves through the environment, it impacts aquatic ecosystems, but at the same time, these ecosystems can naturally attenuate contaminated waters via acid neutralization and catalyzing metal precipitation. This is the case in the former Ronneburg uranium-mining district, where AMD impacts creek sediments. We isolated and characterized two iron-oxidizing *Thiomonas* species that are mildly acidophilic to neutrophilic and that have two genetic pathways for iron oxidation. These *Thiomonas* species are well positioned to naturally attenuate AMD as it discharges across the landscape.

KEYWORDS *Thiomonas*, acid mine drainage, *cyc2*, heavy metals, iron oxidation, pangenome

Citation Akob DM, Hallenbeck M, Beulig F, Fabisch M, Küsel K, Keffer JL, Woyke T, Shapiro N, Lapidus A, Klenk H-P, Chan CS. 2020. Mixotrophic iron-oxidizing *Thiomonas* isolates from an acid mine drainage-affected creek. *Appl Environ Microbiol* 86:e01424-20. <https://doi.org/10.1128/AEM.01424-20>.

Editor Shuang-Jiang Liu, Chinese Academy of Sciences

Copyright © 2020 American Society for Microbiology. All Rights Reserved.

Address correspondence to Denise M. Akob, dakob@usgs.gov, or Clara S. Chan, cschan@udel.edu.

* Present address: Felix Beulig, Universität Bayreuth, Lehrstuhl für Ökologische Mikrobiologie, Bayreuth, Germany.

Received 15 June 2020

Accepted 30 September 2020

Accepted manuscript posted online 2 October 2020

Published 24 November 2020

Acid mine drainage (AMD) is a source of widespread environmental contamination due to low pH and high metal and metalloid concentrations resulting from human mining activities and natural processes. Microbes, particularly iron-oxidizing bacteria (FeOB), are active players in the formation and attenuation of AMD and its associated contaminants (1–5). The roles and identities of FeOB are well established at extremely acidic sites where AMD originates, e.g., Iron Mountain, CA (4–8). However, as AMD moves through the environment via groundwater or surface water, it neutralizes, and the pH becomes moderately acidic to neutral. In this pH range, microbial Fe(II) oxidation can slow metal/metalloid transport via coprecipitation and adsorption to Fe(III) oxide minerals (4, 9–11). Given the likely importance of microbial iron oxidation in moderately acidic AMD environments, characterizing the organisms at such sites is key to understanding remediation mechanisms.

Members of the genus *Thiomonas* (*Betaproteobacteria*) are known to play a role in natural attenuation of AMD contaminants by oxidizing arsenic (As) and are usually grown as mixotrophic sulfur oxidizers (12). *Thiomonas* spp. have been isolated at a range of pH values from moderately acidic to neutral (13–16), and they may have the metabolic potential to catalyze iron oxidation, but associated evidence tends to be equivocal or inconsistent. *Thiomonas delicata* b6^T, isolated from AMD-impacted sediment at the former Cheni gold mine site in Limousin, France, oxidized Fe(II) in medium where thiosulfate was also present (14). *Thiomonas* spp. isolated from the Carnoules mine tailing AMD site (located near Alés, France) have shown variable evidence of Fe(II) oxidation (17, 18). The Carnoules *Thiomonas* sp. strains B1 (AJ549218), B2 (AJ549219), and B3 (AJ549220) were shown to grow and oxidize Fe(II) in mineral medium with thiosulfate and Fe(II) as the energy sources (18). However, the strains were unable to grow in mineral medium with only Fe(II) as an energy source, nor were they able to oxidize iron in creek water from the Carnoules AMD site (18). Another Carnoules strain, *Thiomonas arsenitoxydans* 3As^T, grew on ferrous iron-thiosulfate-tryptone soya broth medium and formed colonies with iron oxide-stained centers (19). However, further tests with strain 3As^T, including cultivation in a fixed-pH (3.2) bioreactor culture and a cell suspension at pH 3.0 or 3.5, indicated that the strain did not oxidize Fe(II) (19). Culturing organisms as iron oxidizers can be difficult, so lack of iron oxidation activity does not necessarily indicate an organism's lack of capability. Instead, the results suggest that *Thiomonas* can oxidize Fe(II) under certain conditions but may require non-Fe(II) additions to mineral media. The widespread occurrence of *Thiomonas* in AMD-impacted environments and its potential to contribute to attenuation of AMD-derived metals and metalloids via Fe(III) precipitation highlight the need to further investigate its Fe oxidation capabilities and mechanisms.

Here, we describe the isolation, physiological characterization, and genomic analyses of two new iron-oxidizing *Thiomonas* species: *Thiomonas ferrovorans* FB-6 and *Thiomonas metallidurans* FB-Cd. The strains were isolated from iron-rich, slightly acidic (pH 6.3) sediments from Gessen Creek in the former uranium-mining district of Ronneburg (Thuringia, Germany), where heavy metals are naturally attenuated via coupled microbial iron cycling and metal precipitation (20, 21). The Ronneburg FeOB strains FB-6 and FB-Cd are unique among *Thiomonas* isolates in that they were isolated on ferrous iron. We conducted a pangenomic analysis of the Ronneburg FB strains and 12 previously sequenced *Thiomonas* isolates and show that the FB strains represent the most genetically distinct members of the genus *Thiomonas*. The FB strains possess genes for two putative Fe(II) oxidation mechanisms, one or both of which they may use to oxidize iron *in situ* and to contribute to natural remediation of heavy metals in the Ronneburg AMD.

(This research was conducted in partial fulfillment of the requirements for undergraduate and graduate degrees for Michelle Hallenbeck, Felix Beulig, and Maria Fabisch. Michelle Hallenbeck conducted the work in partial fulfillment of the requirements for an undergraduate honors degree with distinction from the University of Delaware [22]. Felix Beulig conducted the work in partial fulfillment of the requirements for a master's degree from the Friedrich-Schiller University Jena [23]. Maria Fabisch conducted the

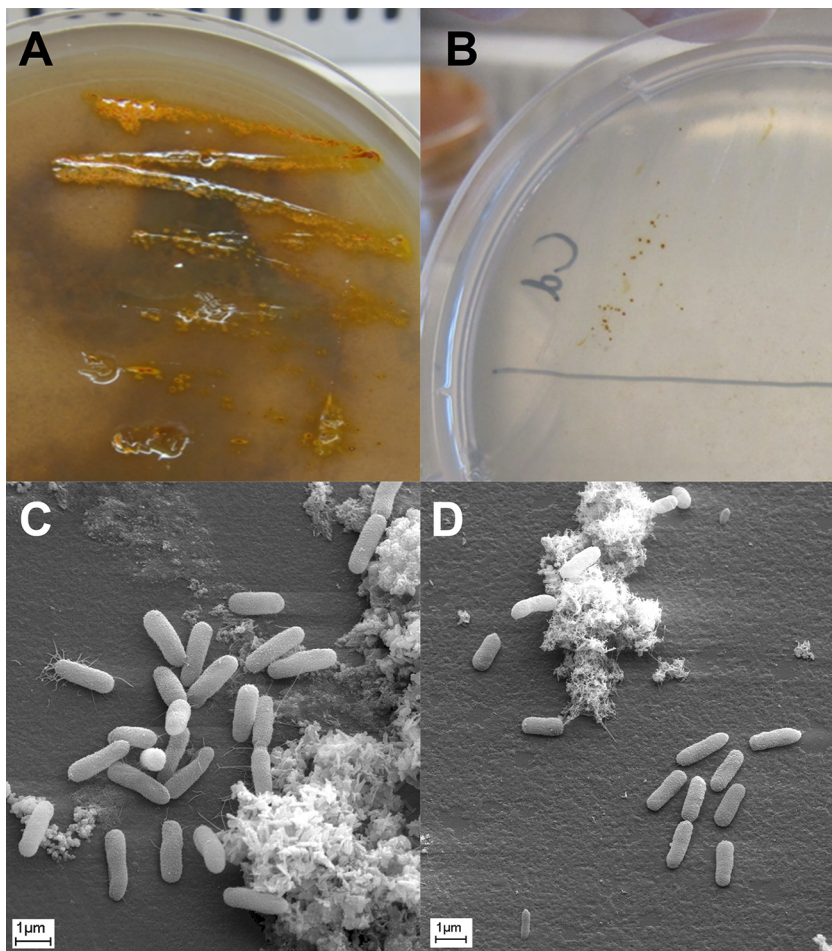


FIG 1 Photographs (A and B) and SEM images (C and D) of FeOB strains FB-6 (A and C) and FB-Cd (B and D). The photographs show growth on FeCO_3 plates; the plates for FB-Cd were amended with 10 mM Cd.

work in partial fulfillment of the requirements for a doctoral degree from the Friedrich Schiller University Jena [24].)

RESULTS AND DISCUSSION

Characterization of iron-oxidizing *Thiomonas* from AMD-affected Gessen Creek sediment. (i) **Isolation of iron oxidizers from AMD-affected Gessen Creek sediment.** Isolates FB-Cd and FB-6 were obtained using a newly developed solid medium for acidotolerant microaerobic iron oxidizers that contained FeCO_3 as an Fe(II) source; plates for isolate FB-Cd also contained 10 mM Cd. The isolates were derived from high-dilution enrichment cultures, indicating that the strains are abundant in creek sediments (20). Single colonies appeared after 1 to 3 weeks and had a maximum diameter of 1 mm (Fig. 1). Scanning electron microscopy (SEM) revealed that strain FB-Cd and FB-6 cells had a short, straight, rod-shaped morphology with cell lengths and diameters of approximately 2 and $0.6 \mu\text{m}$ (Fig. 1). Both strains precipitated iron, as indicated by the orange, rust-colored colonies, showing that they are microaerophilic FeOB (Fig. 1). When transferred to FeCO_3 liquid medium after 2 weeks, the culture formed more orange precipitates than the uninoculated controls (see Fig. S1 in the supplemental material). X-ray diffraction (XRD) analysis of the precipitates confirmed that they are Fe(III)-(oxy)hydroxides of mainly amorphous or nanocrystalline material, including lepidocrocite, goethite, and magnetite (see Fig. S2 in the supplemental material).

(ii) **Identification of *Thiomonas* isolates FB-6 and FB-Cd.** Phylogenetic analysis of 16S rRNA gene sequences revealed that strains FB-Cd and FB-6 were affiliated with the

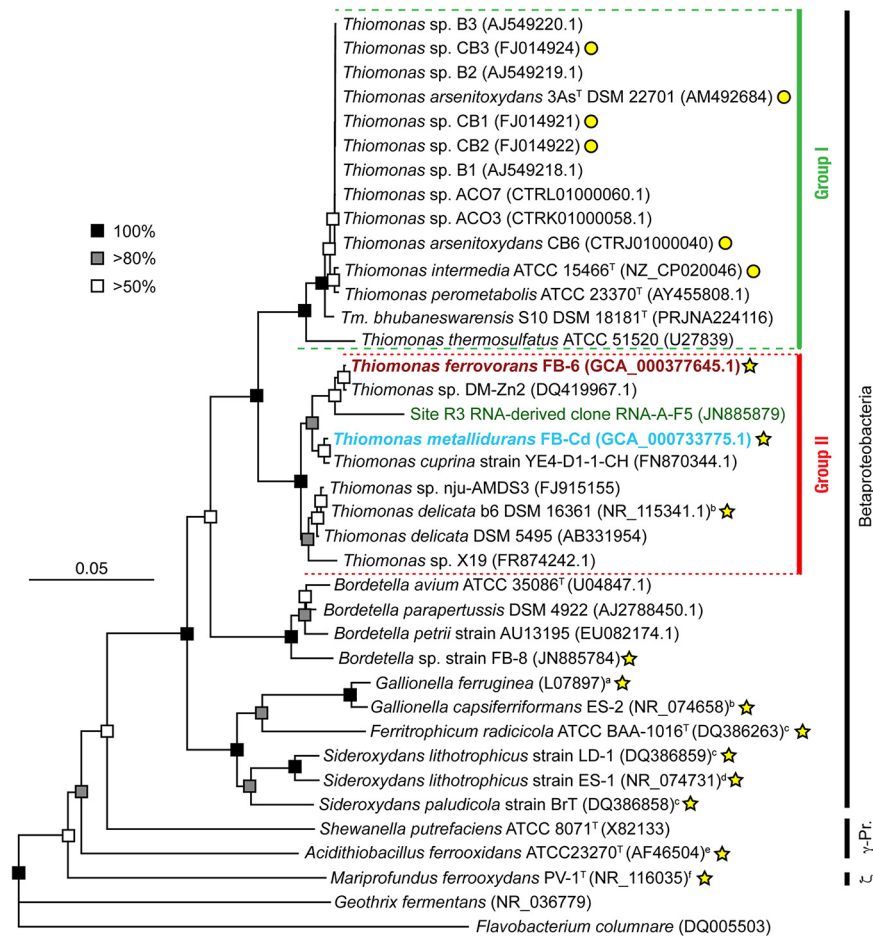


FIG 2 Phylogenetic tree of 16S rRNA gene sequences showing the relationship of the Ronneburg FeOB strains FB-6 and FB-Cd (boldface) to selected representatives from the classes *Betaproteobacteria* and *Gammaproteobacteria*. Clone RNA-R3-F5 (green) was derived from a sediment R3 16S rRNA clone library (20). Known FeOB are indicated by stars, whereas *Thiomonas* strains with varying or inconclusive results for iron oxidation are indicated by circles (see Table 1 for references). GenBank sequence accession numbers are shown in parentheses. The tree represents a consensus of the phylogenies determined using neighbor joining and maximum likelihood. Bootstrap values are shown by the squares, as indicated. The scale bar shows 0.05 change per nucleotide position. *Flavobacterium columnare* was used as the outgroup. a, Hallbeck et al. (84); b, Emerson et al. and Emerson and Moyer (47, 57); c, Weiss et al. (85); d, Emerson and Floyd and Emerson and Moyer (57, 86); e, Temple and Colmer (87); f, Emerson et al. and Chan et al. (88, 89).

genus *Thiomonas* in the order *Burkholderiales* of the class *Betaproteobacteria* (Fig. 2). Phylogenetic analysis of the 16S rRNA genes also clearly displayed two distinct phylogenetic groups within the genus *Thiomonas* (Fig. 2), which have been previously referred to as group I and group II (13, 25, 26). The isolates were found to have a large phylogenetic distance from well-known FeOB, such as *Gallionella ferruginea* (85.8% sequence identity), *Ferritrophicum radicolica* (85.7% sequence identity), *Sideroxydans lithotrophicus* (88.6% sequence identity), and *Acidithiobacillus ferrooxidans* (81.1% sequence identity) (Fig. 2).

The genus *Thiomonas* at present comprises seven species, which largely originate from moderately acidic mining sites (1, 14, 15, 19, 27). Strain FB-Cd shows 99.6% 16S rRNA gene sequence similarity to *T. delicata* strain YE4-D1-1-CH, isolated from the sediment of an acidic coal mine lake in Germany, and tested negative for iron oxidation (28). Strain FB-Cd showed high sequence similarity to other *Thiomonas* strains, *T. delicata* DSM 17897^T, b6 (formerly "*Thiomonas arsenivorans*"), and DSM 5495 (formerly "*Thiomonas cuprina*") (each 97.6 to 98.5% sequence similarity). *T. delicata* strain b6, *Thiomonas intermedia*, and *Thiomonas perometabolis* (14, 29) are known iron-oxidizing

strains and shared 98.5, 93.2, and 93.3% sequence similarity with FB-Cd, respectively. The 16S rRNA gene sequence of isolate FB-6 is 100% identical to those of *Thiomonas* sp. strains DM-Zn2, DM-Ni4, DM-Ni3, DM-Co4, DM-Cd6, DM-Cd5, and DM-Cd4 (unpublished data) (GenBank accession numbers [DQ419961.1](#) to [DQ419967.1](#)), which were isolated as heavy-metal-resistant bacteria from abandoned pyrite mine drainage but not studied in more detail. Strain FB-6 showed high sequence similarity to other *Thiomonas* strains, such as *T. delicata* strains DSM 17897^T, DSM 5495, and YE4-D1-1-CH (97.6 to 97.7%) (Fig. 2). However, according to criteria established by Konstantinidis et al. (30), the FB strains are two separate species, as they share less than 98.6% 16S rRNA gene identity with each other and with the other characterized *Thiomonas* isolates (see Table S3 in the supplemental material). This is further supported by genomic analysis, as discussed below. For these two novel species, we propose the names *Thiomonas ferrovorans* FB-6 and *Thiomonas metallidurans* FB-Cd.

(iii) Physiological characterization of *Thiomonas* isolates FB-6 and FB-Cd. *Thiomonas* spp. are usually grown as facultative chemolithoautotrophs on reduced-sulfur compounds, with optimal growth under mixotrophic conditions at pHs between 3 and 6 (14, 18, 19, 29, 31). Strain FB-Cd was able to grow on thiosulfate and elemental sulfur, whereas strain FB-6 was able to grow only using elemental sulfur (see Table S1 in the supplemental material). The FB isolates showed autotrophic, microaerobic growth with simultaneous Fe(III) precipitation in FeCO₃ liquid medium without an organic carbon source or thiosulfate. More Fe(III) precipitates were observed in autotrophic Fe(II) liquid cultures than in abiotic controls (see Fig. S1). Additionally, we did not observe a pH increase in Fe(III)-stained colonies compared to the surrounding medium (the pH was 5.5 in both cases). These observations suggest that the FB isolates were directly oxidizing iron.

The FB strains were tested for heterotrophic growth with diverse organic compounds, and FB-6 was capable of growth with fructose and pyruvate, while FB-Cd grew with fructose and yeast extract (see Table S1). The ability of the strains to grow on complex carbon and via autotrophy suggests that they are mixotrophic. As we transferred the cultures, it was difficult to maintain growth under autotrophic conditions. We observed consistent growth and iron oxidation in the cultures when the medium was amended with the original sediment extract. As the sediment extract contained dissolved organic carbon (DOC), this lends further support to the mixotrophic nature of the strains. This observation is consistent with the strains being sediment derived, as sediments are complex environments that are likely to contain undefined components that are required for sustained iron oxidation.

Strain FB-6 grew only at pH 5, whereas FB-Cd grew over a pH range of 3.0 to 6.0 (Table 1; see Table S1). Strain FB-Cd was tolerant of 10 mM Cd, while both strains tolerated a mixture of 10 mM Ni, 2.5 mM Cu, 2 mM Cd, 2 mM Co, and 22 mM Zn. *T. delicata* strain DSM 5495, closely related to FB-Cd and FB-6 (98% 16S rRNA gene sequence identity), is known to tolerate 0.9 mM Cd, 7.9 mM Cu, 150 mM Zn, 170 mM Ni, and 850 mM Co (27). *Thiomonas* sp. strains DM-Zn2, DM-Ni4, DM-Ni3, DM-Co4, DM-Cd6, DM-Cd5, and DM-Cd4, which share 100% 16S rRNA gene sequence identity with strain FB-6, were isolated as heavy-metal-resistant bacteria. Similarly, FeOB enrichment cultures from Gessen Creek sediment, the source of the isolates, tolerated up to 34 mM Co, 24 mM Ni, and 1 mM Cd, which were mainly adsorbed to microbially formed iron oxides (20), indicating a mechanism for natural attenuation.

Genome features of strains FB-6 and FB-Cd. The FB-6 and FB-Cd genomes consist of 8 and 6 contigs and are 99.3 and 98.6% complete, respectively (Table 2). At 4.28 and 4.39 Mb, they are larger than the average *Thiomonas* genome size (3.85 Mb; range, 3.20 to 4.64 Mb) and are at either end of a 62.5 to 69.9% GC content range (average, 64.6%) for *Thiomonas* (Table 2). FB-6 and FB-Cd have two 16S-5S-23S rRNA gene operons. The two FB-6 16S rRNA gene sequences are identical to each other, and the two FB-Cd 16S rRNA gene sequences are nearly identical, differing by only one additional guanine residue.

TABLE 1 Metabolic characteristics of Ronneburg isolates FB-6 and FB-Cd and characterized relatives in the genus *Thiomonas*

| Organism | Strain | Culture collection no. | Isolation source | pH range | Temp (°C) | Growth in ^a : | | | Heavy-metal tolerance ^c | Reference(s) |
|-----------------------------------|------------------|------------------------|------------------------------|-----------------------------------|---------------------|--------------------------|---------|---------------------------------------|------------------------------------|--------------------------|
| | | | | | | Fe(II) | As(III) | Reduced-sulfur compounds ^b | | |
| <i>T. ferrovarans</i> | FB-6 | DSM 25805 | AMD sediment | 5.0 | 22 | + | ND | + | Mixture | This study |
| <i>T. metallidurans</i> | FB-Cd | DSM 25617 | AMD sediment | 3.0–6.0 | 22 | + | ND | + | Cd, Mixture | This study |
| <i>Thiomonas</i> sp. | X19 | NA ^d | AMD sediment | 9.8 | 25 | ND | + | ND | ND | 25, 26 |
| <i>T. delicata</i> | b6 ^T | DSM 16361 | AMD sediment | 4.0–7.5 | 20–30 | + | + | + | ND | 14, 31, 90–93 |
| <i>T. bhubaneswarensis</i> | S10 ^T | DSM 18181 | Hot spring sediment | 6.0–8.5 | 25–45 | ND | ND | + | ND | 94, 95 |
| <i>T. intermedia</i> | K12 | NA | Corroded concrete sewer wall | 5.0 | 30 | ND | + | + | ND | 13, 16, 96–98 |
| <i>T. intermedia</i> ^T | Type | ATCC 15466 | Freshwater stream bank mud | 5.5–6.0 | 30–35 | ? | + | + | ND | 14, 19, 93, 99, 100, 101 |
| <i>Thiomonas</i> sp. | CB3 | NA | AMD water | Isolated at 7.0–7.2; grows at 5.0 | 30 | ? | + | + | ND | 16, 17, 18, 102, 103 |
| <i>Thiomonas</i> sp. | CB2 | NA | AMD water | Isolated at 7.0–7.2; grows at 5.0 | 30 | ? | + | + | ND | 16, 17, 18, 102, 103 |
| <i>Thiomonas</i> sp. | ACO3 | NA | AMD sediment | 5.0 | 30 | ND | + | ND | ND | 16, 102 |
| <i>Thiomonas</i> sp. | ACO7 | NA | AMD sediment | 5.0 | 30 | ND | + | ND | ND | 16, 103 |
| <i>Thiomonas</i> sp. | CB1 | NA | AMD water | Isolated at 7.0–7.2; grows at 5.0 | 30 | ? | + | + | ND | 16, 17, 18, 102, 103 |
| <i>Thiomonas</i> sp. | CB6 | NA | AMD water | 5.0 | 30 | ? | + | ND | ND | 16, 17, 102 |
| <i>T. arsenitoxidans</i> | 3As ^T | DSM 22701 | AMD water | 5.0 | 25–37 (optimum, 30) | ? | + | + | ND | 15, 19, 91, 104, 105 |

^aGrowth for a given compound is indicated by +; ND, not determined; ?, unknown. Additional details on the metabolic capacity of the FB isolates are shown in Table S1.

^bGrowth was tested on the following reduced-sulfur compounds: thiosulfate, tetrathionate, and elemental sulfur.

^cGrowth in the presence of Ni (10 mM), Co (10 mM), Cd (10 mM), or a mixture of the three metals was assessed.

^dNA, not applicable.

TABLE 2 Characteristics of *Thiomonas* isolate genomes

| Organism | Strain | GenBank genome accession no. | Genome size (Mb) | % completeness | No. of contigs | GC content (%) | No. of gene clusters | No. of strain-specific gene clusters |
|-----------------------------------|------------------|------------------------------|------------------|----------------|----------------|----------------|----------------------|--------------------------------------|
| <i>T. ferrovorans</i> | FB-6 | GCA_000377645.1 | 4.28 | 99.3 | 8 | 70 | 3,679 | 1,393 |
| <i>T. metallidurans</i> | FB-Cd | GCA_000733775.1 | 4.39 | 98.6 | 6 | 63 | 3,943 | 1,181 |
| <i>Thiomonas</i> sp. | X19 | GCA_900089495.1 | 4.64 | 98.6 | 11 | 65 | 3,924 | 937 |
| <i>T. delicata</i> | b6 | GCA_900088825.1 | 3.84 | 100.0 | 58 | 66 | 3,409 | 532 |
| <i>T. bhubaneswarensis</i> | S10 ^T | GCA_001418255.1 | 3.20 | 98.6 | 25 | 65 | 3,010 | 337 |
| <i>T. intermedia</i> | K12 | GCA_000092605.1 | 3.34 | 99.3 | 2 | 65 | 3,058 | 8 |
| <i>T. intermedia</i> ^T | Type | GCA_002028405.1 | 3.34 | 99.3 | 2 | 65 | 3,053 | 2 |
| <i>Thiomonas</i> sp. | CB3 | GCA_900004415.1 | 4.33 | 100.0 | 65 | 64 | 3,618 | 230 |
| <i>Thiomonas</i> sp. | CB2 | GCA_000947035.1 | 3.74 | 100.0 | 92 | 64 | 3,369 | 153 |
| <i>Thiomonas</i> sp. | ACO3 | GCA_900004955.1 | 3.61 | 100.0 | 65 | 64 | 3,315 | 3 |
| <i>Thiomonas</i> sp. | ACO7 | GCA_900004405.1 | 3.66 | 100.0 | 68 | 64 | 3,327 | 4 |
| <i>Thiomonas</i> sp. | CB1 | GCA_900005065.1 | 3.88 | 100.0 | 31 | 64 | 3,471 | 12 |
| <i>Thiomonas</i> sp. | CB6 | GCA_900004565.1 | 3.81 | 100.0 | 43 | 64 | 3,420 | 6 |
| <i>T. arsenitoxidans</i> | 3As ^T | GCA_000253115.1 | 3.79 | 100.0 | 3 | 64 | 3,409 | 24 |

To understand the relationships between and among the strains, we compared the genomes of the 14 *Thiomonas* isolates by 16S rRNA gene identities (see Table S3), average nucleotide identity (ANI) (Fig. 3A; see Table S4 in the supplemental material), average amino acid identity (AAI) (Fig. 3B; see Table S5 in the supplemental material), and concatenated ribosomal protein phylogeny (see Fig. S3B in the supplemental material). Using the criteria of Konstantinidis et al. (30), organisms in the same genera should possess 65 to 95% AAI and 95 to 98.6% 16S rRNA gene identity. The 16S rRNA gene identity cutoff clearly suggests that all four group II organisms (FB-6, FB-Cd, X19, and b6) should be in their own genus, different from the group I organisms. However, the AAI analysis is less clear about the genus division, with the FB-6 AAI values (63.3 to 64.2% identity to group I) suggesting it belongs in a separate genus from the other group I organisms, while the AAI values for FB-Cd, X19, and b6 do not support this delineation (66.9 to 70.8% identity to group I). Since a strict interpretation of the cutoff values is ambiguous in this case, for now, we recommend that all the strains remain in the genus *Thiomonas*. The FB strains clearly represent unique species (<95% ANI, <95% AAI, and <98.6% 16S rRNA gene identity) and thus have been given new species names (*T. ferrovorans* FB-6 and *T. metallidurans* FB-Cd). Taken together, these analyses clearly show that the newly isolated FB strains are the most distantly related members of the genus *Thiomonas*.

***Thiomonas* isolate pangenome.** To identify a *Thiomonas* core genome and to determine which gene clusters were shared by subsets of the genus, we conducted a pangenome analysis for all 14 *Thiomonas* isolates with genome sequences (Fig. 4). Here, a gene cluster is defined as a set of homologous genes found in one or more genomes. The core gene set for all 14 *Thiomonas* genomes was composed of 1,296 gene clusters. The FB strains have the largest numbers of strain-specific gene clusters (1,181 for FB-Cd and 1,393 for FB-6) (Fig. 4 and Table 2), making them the most genetically diverse of the *Thiomonas* isolates, consistent with their phylogenetic distinctiveness (Fig. 2; see Fig. S3). The group I *Thiomonas* strains have fewer strain-specific gene clusters and more group-specific gene clusters than group II strains (Fig. 4), which is not unexpected, since the number and the relatedness of the isolates in group I are higher than in group II.

Only 19 gene clusters were specific for AMD-derived isolates (Fig. 4), and none appeared to have a function associated with tolerance for conditions associated with AMD. However, some metal resistance genes were present in only a subset of the AMD isolates or were shared by all *Thiomonas* isolates regardless of whether they were isolated from AMD. The arsenite oxidase genes *aioAB* were present in all AMD-derived strains but FB-6 and in two of the three non-AMD strains (K12 and *T. intermedia*^T). Additionally, the core genome had several gene clusters involved in cobalt-zinc-cadmium resistance, as well as metal ion efflux pumps. Evidently, the genetic potential

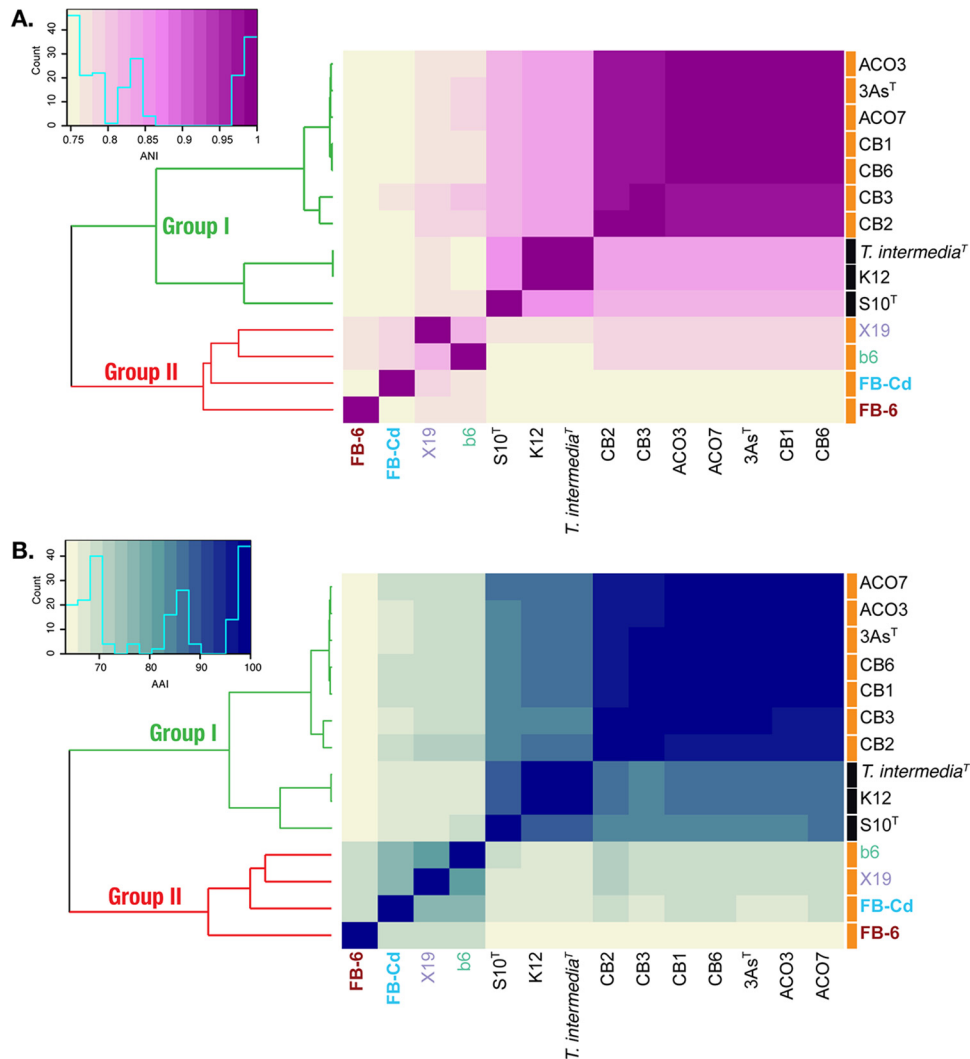


FIG 3 Heat map of the ANI (A) and AAI (B) for the 14 *Thiomonas* isolate genomes. The dendrograms showing similarity between the genomes are color coded to indicate whether the *Thiomonas* strains belong to group I (green) or group II (red). Sources of isolates are indicated by orange and black boxes for AMD and non-AMD environments, respectively.

for heavy-metal resistance is not characteristic of only the AMD-derived isolates, but instead is common to all *Thiomonas* isolates.

Fe(II) oxidation pathways in *Thiomonas*. We identified two possible Fe(II) oxidation mechanisms within the *Thiomonas* isolate genomes: the putative iron oxidation genes *mtoAB* and the potential iron oxidase gene *cyc2*. Homologs of *cyc2* were found in all the strains except *T. intermedia*^T, whereas *mtoAB* was found only in the FB strains (see Table S6 in the supplemental material for locus tags). In addition, we found possible components of complete aerobic iron oxidation pathways (Fig. 5), including reverse electron transport and two heme biosynthesis pathways.

The *mtoAB* sequences are homologous to the iron reductase genes *mtrAB*, which were initially characterized in iron-reducing bacteria like *Shewanella* (33) but are named *mto* rather than *mtr* to distinguish sequences found in iron oxidizers from those in iron reducers. An initial search for potential iron oxidation mechanisms in the iron oxidizer *S. lithotrophicus* ES-1 identified a gene cluster (Slit_2495-Slit_2498) that contained homologs of the *Shewanella* decaheme cytochrome gene *mtrA*; an outer membrane porin gene, *mtrB*; and a tetraheme quinol oxidoreductase gene, *cymA* (34), as well as an additional monoheme cytochrome gene named *mtoD* (35).

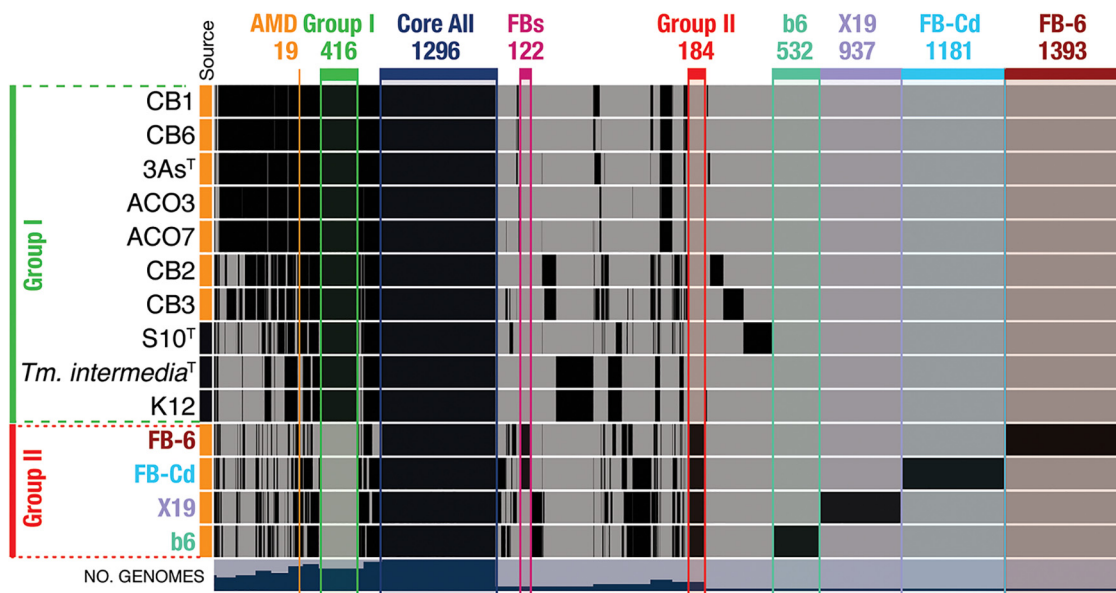


FIG 4 Overview of the *Thiomonas* isolate pangenome generated with Anvi'o v5.1. The columns represent gene clusters, with black indicating the presence of a gene cluster in a genome. The numbers indicate the number of strain- or group-specific gene clusters. The FB strains have the largest numbers of strain-specific gene clusters, followed by the other two members of group II. Additionally, there are very few gene clusters specific to the AMD-derived isolates (orange).

Characterization of MtoA_{ES-1} demonstrated Fe(II) oxidation *in vitro* under some conditions and thus provided support to the hypothesis that *mtoAB* performed iron oxidation functions (34). To assess whether the FB strain genes were more similar to *mtoAB* or *mtrAB*, we constructed a phylogenetic tree of concatenated MtoAB-MtrAB sequences from the *Thiomonas* FB genomes, known iron oxidizers and reducers, and a few other related sequences (see Fig. S4A in the supplemental

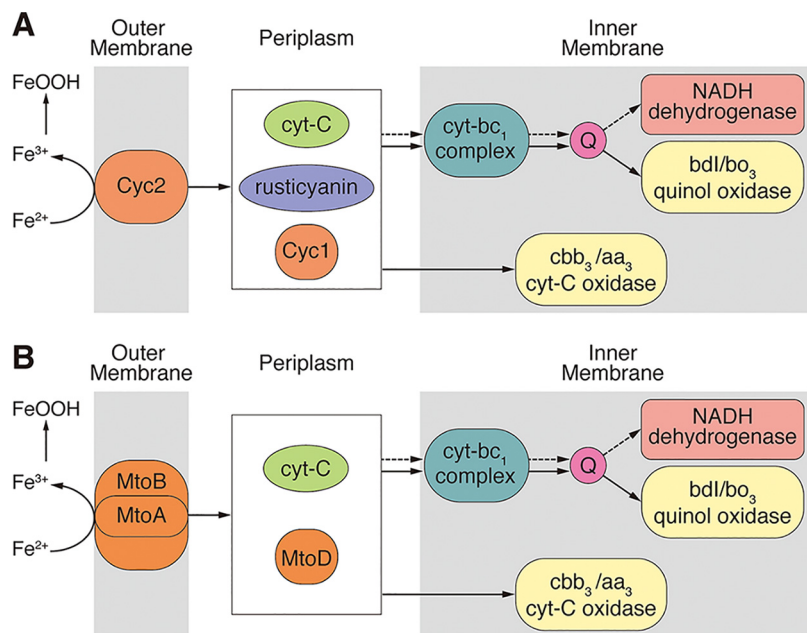


FIG 5 Schematic diagram of the hypothetical Cyc2-based (A) and MtoA-based (B) iron oxidation pathways in *T. ferrovorans* FB-6 and *T. metallidurans* FB-Cd. Electrons are transported from Fe²⁺ to the electron transport chain via an outer membrane cytochrome, to periplasmic proteins, to terminal oxidases on the inner membrane. Reverse electron transport is indicated by dashed arrows. Cyt and cyt-C, cytochrome c. Q represents the quinone pool. The *bo*₃ quinol oxidase is found only in strain FB-6.

material). The FB strain sequences are more closely related to those of known iron oxidizers (42 to 45% identity to *MtoAB*_{ES-1}) than to those of known iron reducers, providing support for a possible role in iron oxidation (33, 36). In both FB genomes, *mtoAB* is flanked by a gene encoding a small monoheme cytochrome (108 or 121 amino acids [aa]). While the genetic arrangement suggests this represents the periplasmic cytochrome *MtoD*, there are other cytochrome genes in all of the *Thiomonas* isolate genomes that share higher sequence identity to *mtoD*_{ES-1}. None of the *Thiomonas* isolate genomes contain a homolog of the tetraheme inner membrane cytochrome gene *cymA*, which is an essential part of *mtr* pathways and part of the *mto* cluster in the ES-1 genome.

In contrast to *mtoAB*, almost all *Thiomonas* genomes include *cyc2*, with the exception of that of *T. intermedia*^T. The *Thiomonas* Cyc2 tree is generally congruent with that of the concatenated ribosomal protein tree, with sequences separating into groups I and II and similar branching orders and relative branch lengths (see Fig. S4B). This suggests that *cyc2* was inherited vertically. Cyc2 is a fused monoheme cytochrome and porin, with the cytochrome region more highly conserved (37). Indeed, the conserved cytochrome regions of the FB strain Cyc2 sequences have 45.5 to 54.7% identity with that of the *A. ferrooxidans* ATCC 23270 Cyc2 cytochrome region, while the less conserved porin regions have 30.2 to 30.9% identity with that of *A. ferrooxidans* Cyc2 (UniProt accession no. B7JJAQ7). Despite sequence homology, the genomic environment surrounding *cyc2* in the *Thiomonas* strains is not the same as in *A. ferrooxidans* ATCC 23270. In *A. ferrooxidans*, *cyc2* is found in an operon with a periplasmic diheme cytochrome gene, *cyc1*; a periplasmic copper-binding protein, rusticyanin; and a terminal oxidase, all of which likely play roles in aerobic iron oxidation (38). In the *Thiomonas* genomes, *cyc2* is adjacent to genes encoding several small proteins, but none of them are redox active components. In most of the *Thiomonas* genomes, there are one or two diheme cytochromes with >30% identity to Cyc1_{A.ferrr} but none are collocated with other electron transport genes. A rusticyanin homolog (34 to 35% identity to Rus_{A.ferrr}) is present in four *Thiomonas* genomes, including both FB strains, but the gene is not near other iron oxidation pathway genes (see Table S6). The FB strain genomes include genes that encode proteins with the CXXCH/CXXXCH heme-binding motif (see Table S7 in the supplemental material), some of which may also play roles in bioenergetic electron transport.

A periplasmic cytochrome(s) can pass electrons to a terminal oxidase; the FB genomes encode *bdI* ubiquinol oxidase, and both *cbb*₃-type and *aa*₃-type cytochrome *c* oxidases, which generate proton motive force. FB-6 also has a *bo*₃ quinol oxidase. All 14 isolates have both *cbb*₃- and *aa*₃-type terminal oxidases, except strain X19, which has only the *aa*₃ type. The *cbb*₃ type is adapted to low O₂, while the *aa*₃ type is adapted to high O₂ (39), suggesting that most *Thiomonas* strains can tolerate a wide range of O₂ concentrations. To grow by iron oxidation, FB-6 and FB-Cd need reverse electron transport to generate reducing power. We were able to reconstruct hypothetical iron oxidation pathways from the genomes of both FB strains (Fig. 5; see Table S6). Because the redox potential of Fe²⁺/ferrihydrite is close to zero at neutral pH (−100 mV to +100 mV) (40) and even higher at acidic pH, iron oxidizers require reverse electron transport to generate NADH for carbon fixation and other biosynthesis reactions. This may be accomplished by directing electrons to the cytochrome *bc*₁ complex, through the quinone pool, to NADH dehydrogenase (Fig. 5). This model is consistent with the models proposed for other neutrophilic FeOB (37, 41–43), as well as the functionally verified *A. ferrooxidans* model (44, 45). While many other iron oxidizers possess an alternative complex III (ACIII) (46, 47), the complex does not appear to be present in the *Thiomonas* isolate genomes. Considering all the parts of the electron transport system, 13 of the 14 *Thiomonas* isolates have all the components of a Cyc2-based iron oxidation pathway; the exception is *T. intermedia*^T (99.3% genome completeness), which lacks both *cyc2* and *mtoAB* (see Table S6). Our analyses suggest that all of the *Thiomonas* isolates except *T. intermedia*^T may have the genetic potential for iron oxidation using the putative iron oxidase Cyc2.

The presence of two possible iron oxidation genes (*cyc2* and *mtoA*) in the FB strains and their isolation as iron oxidizers suggests that they are metabolically more versatile regarding iron oxidation than the other *Thiomonas* isolates, which possess only *cyc2*. The FB strains are also distinct from other *Thiomonas* strains in having both system I and system II cytochrome *c* biogenesis systems (see Table S6), which transport heme to the periplasm and covalently link it to apocytochromes to form *c*-type cytochromes, such as *Cyc2* and *MtoA* (48). All of the *Thiomonas* isolate genomes possess system II, a two-protein heme channel and cytochrome *c* synthase. However, only the FB strains possess system I, which includes eight or more proteins and requires reducing power and energy from ATP hydrolysis (48). A key feature of the more complex system I is the heme chaperone *CcmE*, which has a high affinity for heme and acts as a heme reservoir (49), which may aid in the assembly of multiheme cytochromes. The FB strain system I genes are encoded in a complete *ccm* operon (48) located almost directly adjacent to *mtoAB*. The unusual possession of both cytochrome biogenesis systems, combined with the fact that the FB strain genomes include both *cyc2* and *mtoAB*, may indicate specialized utilization of the different systems (e.g., *MtoAB* with system I and *Cyc2* with system II) under different growth conditions.

Carbon metabolism. The FB strains have the genetic potential for autotrophy, as indicated by a complete Calvin-Benson-Bassham cycle (see Table S6). Along with the other group II isolates, the FB strains have only genes that encode form I RuBisCO, while the group I strains have both form I and form II RuBisCO genes. Form I is better suited to higher O₂ conditions than form II (50), which could indicate that the group I strains are adapted to a wider range of O₂ concentrations. However, the presence of both *cbb₃*- and *aa₃*-type terminal oxidases in group II strains FB-6, FB-Cd, and b6 indicates that they could still tolerate a wide range of O₂ concentrations, suggesting that there may be other reasons that group II strains have only form I RuBisCO.

The FB strains also have full pathways for the tricarboxylic acid (TCA) cycle and glucose degradation, necessary for central metabolism and utilization of organics (see Table S6). The *Thiomonas* isolate genomes include the glycolysis pathways (Entner-Doudoroff [ED] and Embden-Meyerhof-Parnas [EMP]) and oxidative pentose phosphate (OPP) pathways (see Table S6). All of the *Thiomonas* isolates except b6 and X19 have complete EMP pathways, including the key enzyme phosphofructokinase. All the strains but b6 encode complete ED pathways, including the key enzyme 2-keto-3-deoxy-phosphogluconate (KDPG) aldolase (51). Strains FB-Cd, b6, and X19 are the only strains that have genes for a complete OPP pathway (see Table S6), indicating that, despite the lack of a full EMP and/or ED pathway in these organisms, they can still carry out heterotrophic metabolism. Thus, all the isolates have at least one complete glucose degradation pathway encoded in their genomes, which may be used for mixotrophic or heterotrophic metabolism.

More specific evidence of organic utilization was found by identifying genes for organic transport and uptake. Both FB-6 and FB-Cd can grow on fructose (Table 1), and both have monosaccharide-specific uptake systems. FB-6 has genes for several monosaccharide ABC transporters, while FB-Cd has genes for a complete fructose-specific phosphotransferase system (PTS), which brings fructose into the glycolysis pathway. Genes for a complete fructose PTS are also found in 3As^T, K12, *T. intermedia*^T, the CB strains, and the ACO strains (see Table S6). Genes for many other organic carbon ABC transporters were found in the *Thiomonas* genomes, though not all of them appeared complete (see Table S6). All the strains had complete systems for putrescine transport and branched-chain amino acid transport, encoded by the genes *potFGHI* and *livFG-MHK*, respectively. FB-6 has a wider variety of organic carbon ABC transporters than the other isolates: in addition to monosaccharide transporters, there are systems for other carbohydrates, sorbitol/mannitol (*smoEFGK*), and L-cystine/cysteine transporters (*yecSC* and *fljY*). The presence of organic carbon transporters in the *Thiomonas* genomes, together with the presence of at least one glycolytic pathway, is consistent with the

observation that many of the strains, including FB-6 and FB-Cd, can grow heterotrophically.

Heavy-metal resistance mechanisms. All 14 *Thiomonas* isolates have the genetic potential for heavy-metal resistance, as they possess genes involved in resistance to Co, Zn, Cd, Mg, Ni, Hg, As, and Cr (see Table S6). Both strains FB-6 and FB-Cd have the complete pathways for heavy-metal efflux and resistance (e.g., *czcABCDR* and *cusABR*), which helps explain how they tolerate millimolar concentrations of Ni, Cu, Cd, Co, and Zn (Table 1). The same metal resistance genes are also present in the other *Thiomonas* strains, except b6, *T. intermedia*^T, ACO strains, and X19. Many of the *Thiomonas* genomes include genes that encode chromate and cobalt resistance genes (see Table S6). Most *Thiomonas* isolates (except FB-6 and S10) also have the genetic potential for arsenite oxidation, as they have the genes *ainAB*. All isolates except S10 and *T. intermedia*^T have the mercuric ion reductase gene *merA* for mercury resistance. The majority of isolates harbor mercury transport genes (*merCTP*), except the FB strains, S10, and *T. intermedia*^T.

Implications. In order to understand biogeochemical processes in AMD-contaminated freshwater sediments, detailed knowledge about the composition and the metabolic potential of metal-oxidizing microbial communities is essential. Here, we have described two distinct novel species of *Thiomonas*, for which we propose the names *Thiomonas ferrovorans* FB-6^T sp. nov. and *Thiomonas metallidurans* FB-Cd^T sp. nov. They are the most genetically distinct of all sequenced *Thiomonas* strains, contributing both genetic and metabolic diversity to the genus. The organisms are particularly valuable, as they were isolated and grown as mixotrophic iron oxidizers with broad heavy-metal tolerance. The use of *Thiomonas* spp. for remediation of AMD has been proposed (8, 29), and the coprecipitation of heavy-metal and radionuclide contaminants with biogenic Fe(III) oxides has also been put forth as a bioremediation strategy (52). Our analyses revealed that the FB strains have the genetic potential for iron oxidation by two putative mechanisms (*cyc2* and *mtoAB*), while all other *Thiomonas* isolates carry only *cyc2*. Dual iron oxidation mechanisms may enable the FB strains to be more efficient at iron oxidation or perhaps to oxidize iron under a wider range of conditions, increasing their applicability for bioremediation. Growth and iron oxidation are promoted by undefined sediment-derived components, which is not unexpected for organisms isolated from surficial sediments, and extract amendment could be incorporated into bioremediation schemes. These *Thiomonas* spp. differ from well-known acidophilic Fe oxidizers in that they grow at moderately acidic to nearly neutral pHs. In sum, our combined physiological and genomic characterization suggests that the *Thiomonas* FB strains, and perhaps many *Thiomonas* spp., are mixotrophic iron oxidizers that fill an environmental niche key to AMD remediation: slightly acidic metal- and sulfur-rich sediments that result as AMD waters discharge across landscapes. These results give us a clearer view of how iron-oxidizing *Thiomonas* strains can aid in natural attenuation, as well as engineered remediation solutions for persistent and widespread AMD problems.

MATERIALS AND METHODS

Enrichment and isolation of FeOB. The source environment is located in the former Ronneburg uranium-mining district (Thuringia, Germany). The area is contaminated due to mining activities, uranium recovery with sulfuric acid leaching of low-grade black shale, and pyrite oxidation (53). Despite physical remediation conducted in the 1990s, groundwater and surface waters are still contaminated with heavy metals (20, 54, 55). Enrichment cultures were first established by Fabisch et al. (20), who showed that FeOB were numerically abundant in creek sediment, using a most probable number (MPN) technique (56). Sediment from the slightly acidic site R3 (pH 6.3) was selected for isolation of FeOB, because it showed the highest heavy-metal contamination of the sites studied by Fabisch et al. (20). Site R3 sediment contained 3.2, 2.8, and 6.2 μmol of Ni, Cu, and Zn, respectively, per g dry weight sediment and 3.06 mmol total Fe per g dry weight sediment (20). Sequential extractions of creek sediment showed that a large portion of metals in the sediment (especially Ni, Cu, Zn, Pb, and U) were associated with iron oxides (20). Microaerobic FeOB enrichments were grown in gradient tube cultures (57) modified as described by Lüdecke et al. (32) with an FeS plug and a semisolid agarose-stabilized overlayer. When isolating for FeOB from Gessen Creek, we initiated a number of enrichment cultures, including tubes amended with Ni, Co, or Cd (20); cultures amended with 10 mM CdCl₂ yielded strain FB-Cd. A

water-soluble sediment extract was added to all of the enrichment cultures to select for environmentally relevant strains, because amendment of DOC is known to accelerate biological Fe(II) oxidation (58, 59). The extract contained 26 mg liter⁻¹ DOC and heavy metals in the micromolar range and was added at 1:60 (vol/vol) (20). The cultures were incubated at 22°C in the dark, and active enrichment cultures at the highest dilution factor showing growth were diluted and transferred.

To obtain pure cultures of iron oxidizers, we developed a new plate type, FeCO₃ plates, that contained 10 mM FeCO₃ as a stable ferrous iron source at pH 5.5 (stability was indicated by no visible color changes in the uninoculated control), as described in the supplemental material. Inoculated plates were incubated at room temperature in the dark in anaerobic jars or gas-tight bags (Space Bag, USA) with a micro-oxic headspace of N₂-CO₂-O₂ (85:10:5 [vol/vol/vol]). Colonies were transferred on plates at least 3 times, and after 3 transfers with positive growth, the cultures were assumed to be pure. Microscale pH changes were measured in and around the colonies on agar plates using a pH microelectrode (pH 500; Unisense, Denmark), and the data were recorded with Sensor Trace Basic 1.2 software (Unisense, Denmark).

The pure colonies were transferred to 5 ml FeCO₃ liquid medium (pH 5.5), which has the same composition as FeCO₃ plates but without agarose (prepared using solution A [see methods in the supplemental material], FeCO₃, and vitamin solution only). The tubes were plugged with sterile cotton stoppers to allow gas exchange and cultivated in gas-tight bags at room temperature in the dark with a micro-oxic headspace of N₂-CO₂-O₂ (85:10:5). The cultures were maintained in liquid medium and were the source of biomass for the metabolic assays described below. The FB strains were also grown in complex media, such as lysogeny broth (LB; per liter: 10 g Tryptone, 5 g yeast extract, and 10 g NaCl) and R2A medium (107) (liquid and solid). All isolation work was conducted on a clean bench (biological safety cabinet class 2; Astec-Microflow, United Kingdom).

Scanning electron microscopy of isolates. Isolate morphology was determined using SEM. A subsample of an active culture in FeCO₃ liquid medium was collected on a lysine-coated coverslip by sedimentation, followed by a standard SEM preparation procedure (60). In brief, the cells were fixed with 2.5% glutaraldehyde in cacodylate buffer, and then samples were washed 3 times in cacodylate buffer for 10 min each time. Dehydration took place as a series of steps in which the samples were incubated for 10 min each time in ethanol-water mixtures with increasing ethanol concentrations (15%, 30%, 50%, 70%, 80%, and 90% and two times with 100%). The cells were critical-point dried (CPD 030; BAL-TEC, Liechtenstein). The dried samples were applied to a sample stub and coated with a conductive layer of ~10 nm platinum in a sputter coater (SCD 005; BAL-TEC, Liechtenstein). All the samples were examined with an FE-SEM LEO-1530 Gemini (Carl Zeiss NTS, Germany) at magnifications of ×1,000 to ×20,000 at 10 kV.

16S rRNA gene sequencing and phylogenetic analysis of isolates. DNA was extracted from isolates by resuspending colonies from FeCO₃ plates in 100 μl of 5% Chelex 100 resin (Bio-Rad; catalog no. 142-1253) and then boiling for 10 min. After boiling, the solution was centrifuged at maximum speed for 1 min and stored at 4°C until use. Genomic DNA was PCR amplified using the *Bacteria* domain-specific 16S rRNA gene primers fD1 and rP2 (61). The PCR products were purified using a NucleoSpin Extract II kit according to the manufacturer's instructions and then sent to Macrogen Europe (Amstelveen, Netherlands) for bidirectional sequencing. Sequences were trimmed and contigs were constructed using Geneious Pro Beta 4.7.2 (Biomatters, New Zealand) (62). Closest relatives were identified using the BLAST algorithm (63, 64) against the GenBank database available from the National Center for Biotechnology Information (NCBI) (65). Isolate sequences were then aligned using the Greengenes Align tool and then imported into the greengenes.arb database (66) within the ARB software package (67). A consensus tree was constructed based on neighbor-joining and maximum-likelihood methods, using a LaneMask filter with a Jukes-Cantor correction in ARB.

Screening of metabolic properties of FeOB isolates. Strains were screened for the ability to grow heterotrophically, lithoautotrophically with different energy sources, in the presence of heavy metals, and under different pH conditions in appropriate media. Washed cells from an active iron-oxidizing culture in FeCO₃ liquid medium was used as the inoculum for each assay; the cells were washed three times with sterile, anoxic 0.9% NaCl. Growth was monitored indirectly by optical density measurement at 600 nm (OD₆₀₀). Growth rates and doubling times were calculated from semilogarithmic plots of optical density against time for the exponential-growth phase. As cells in FeCO₃ liquid medium were typically associated with solid-phase iron, growth was determined by enumerating cells using DAPI (4',6'-diamidino-2-phenylindole) direct cell counts. The pH range and optimum of the strains were determined by growth of triplicate cultures in FeCO₃ liquid with the pH adjusted to values of 2 to 8 in steps of 1 pH unit using H₂SO₄ or NaOH. Heterotrophic growth was assessed in medium containing (per liter) 20 ml of 50× basal salts solution (68); 1 ml trace elements solution (69); and 12 mM glucose, fructose, lactate, or pyruvate or 0.12% yeast extract. Lithoautotrophic growth with reduced-sulfur compounds was determined in pH 5.5 medium containing (per liter) 20 ml of 50× basal salts solution; 1 ml trace elements solution; and either 20 mM thiosulfate, 10 mM tetrathionate, or 0.5% elemental sulfur. All the reduced-sulfur compounds were added from sterile anoxic stocks; sulfur was autoclaved and then dispensed using aseptic techniques. Heavy-metal tolerance was determined in FeCO₃ liquid medium amended with 10 mM Ni, 10 mM Co, or 10 mM Cd and a mixture of 10 mM Ni, 2.5 mM Cu, 2 mM Cd, 2 mM Co, and 22 mM Zn. The cultures were incubated at room temperature in the dark and under a micro-oxic headspace of N₂-CO₂-O₂ (85:10:5).

X-ray diffraction analysis of iron precipitates. The mineralogy of the solid phases formed in the liquid cultures was determined using XRD. Samples from liquid cultures were centrifuged (5,000 × *g* for 10 min), and the resulting precipitates were rinsed three times using degassed distilled water to remove

soluble salts and Fe(II). The washed precipitates were dried overnight at 50°C, ground with a mortar, and then dispensed into silicate capillaries before analysis. XRD measurements were performed with CoK α radiation on a Seifert FPM XRD7 diffractometer (Rich.Seifert & Co. GmbH, Germany) mounted in the Debye-Scherrer configuration using 40 kV and 30 mA. Data were recorded in the continuous-scan mode within the 5° to 80° 2 θ range with 10 s per step of 0.02°. The results were compared to those for reference compounds from the American Mineralogist crystal structure database (70).

Genome sequencing and annotation. Isolates FB-6 and FB-Cd were grown to high cell density in heterotrophic media for genome sequencing. FB-6 was cultivated in LB under micro-oxic conditions (85:10:5 N₂-CO₂-O₂), whereas optimal growth for FB-Cd was obtained in R2A medium under fully oxic conditions. The cultures were shaken at 65 rpm and incubated at room temperature in the dark. Following growth, biomass was harvested by centrifugation, frozen at -20°C, and then shipped to the Deutsche Sammlung von Mikroorganismen und Zellkulturen (DSMZ) (Braunschweig, Germany) for DNA extraction. DNA was extracted using the U.S. Department of Energy (DOE) Joint Genome Institute (JGI) cetyltrimethylammonium bromide (CTAB) procedure for isolating high-molecular-weight genomic DNA (<http://my.jgi.doe.gov/index.html>). The DNA was quality controlled using agarose gel electrophoresis to evaluate the quality, quantity, and molecular weight of the extract according to the JGI protocol "Genomic DNA QC Using Standard Gel Electrophoresis" (<http://my.jgi.doe.gov/index.html>).

The draft genome of *Thiomonas* sp. FB-6 was generated at the JGI using a hybrid of Illumina (Illumina, Inc., San Diego, CA) and Pacific Biosciences (PacBio) (73) technologies, as described in the supplemental material. Illumina shotgun and long-insert mate pair (18 kb) libraries were constructed and sequenced using the HiSeq 2000 platform. A PacBio SMRTbell library was constructed and sequenced on the PacBio RS platform (Pacific Biosciences, Menlo Park, CA). All raw Illumina sequence data were passed through the DUK filtering program (71). Filtered Illumina and PacBio reads were assembled using AllpathsLG version R37654 (72). The final draft assembly contained 8 contigs (contig N_{50}/L_{50} 1/3.0 Mb) in 8 scaffolds (scaffold N_{50}/L_{50} 1/3.0 Mb), with a total genome size of 4.3 Mb. The final assembly is based on 3,197.6 Mb of Illumina standard paired-end (PE), 4,867.2 Mb of Illumina Cre-LoxP inverse PCR (CLIP) PE, and 356.6 Mb of PacBio postfiltered data, which provided average 1,875.5 \times Illumina and 82.9 \times PacBio coverage of the genome, respectively.

The draft genome of *Thiomonas* sp. FB-Cd was generated at the JGI using PacBio sequencing technology (73), as described in the supplemental material. PacBio sequencing generated 221,970 filtered subreads totaling 631.8 Mbp, which were assembled using HGAP version 2.1.1 (74). The final draft assembly contained 6 contigs (N_{50} 2.8 Mbp) in 6 scaffolds, totaling 4.4 Mbp, with a read coverage of 217.1 \times .

Thiomonas genome comparisons. Twelve other *Thiomonas* isolate genomes (Table 2; see Table S2 in the supplemental material) were acquired from the NCBI database (65). Genome completeness was estimated using Anvi'o v5.1 (75). All 14 genomes, including FB-6 and FB-Cd, were uploaded to the Rapid Annotations based on Subsystem Technology (RAST) prokaryotic genome annotation server for annotation (76). The genomes were also submitted to BlastKOALA for KEGG annotation (106). KEGG metabolic pathways in IMG were used to identify key energy metabolisms and related genes in the genomes, and RAST was used to browse the genomes for genes of interest, in particular genes unique to the FB strain genomes with respect to other *Thiomonas* isolates.

Nucleotide and protein sequence alignments were generated in Geneious (v. 10.1.3) (62). Cyc2 sequences were found in the Integrated Microbial Genomes and Microbiomes (IMG/M) database (77) and NCBI databases using BLAST (64) by comparing the Cyc2 sequence from *A. ferrooxidans*. An alignment of the *Thiomonas* Cyc2 protein sequences was produced, which was used to construct a maximum-likelihood tree. The FB strain MtoAB/MtrAB sequences, as well as those of several known iron oxidizers and reducers, were found in the IMG/M and NCBI databases. The FB strain MtoAB homologs were identified by BLAST using the MtoAB sequences from *S. lithotrophicus* ES-1 (34, 47). MtoA/MtrA and MtoB/MtrB protein sequence alignments were generated using MUSCLE and subsequently concatenated. The concatenated alignment was used to generate an MtoAB/MtrAB maximum-likelihood tree. Ribosomal protein sequences in the core genome were identified from the pangenome analysis using the Clusters of Orthologous Groups (COG) annotations assigned to the gene clusters (see below). An alignment was generated for 47 separate ribosomal proteins, including the large-subunit ribosomal proteins L1 to L6, L9 to L11, L13 to L24, L27 to L31, L33, and L35 and the small-subunit ribosomal proteins S2 to S18, S20, and S21. The resulting 47 protein alignments were concatenated and used to generate a maximum-likelihood tree using the RAxML plugin (78) in Geneious (v. 10.1.3) (62).

Anvi'o v5.1 (75) was used to conduct a pangenome analysis of the *Thiomonas* isolates using the Anvi'o pangenomic workflow as described by Delmont and Eren (79). RAST was used to call open reading frames (ORFs), and a contig database was generated for each genome using the command `anvi-gencontigs-database`. The Anvi'o command `anvi-run-ncbi-cogs` was used to annotate the contig databases by NCBI's COG before the pangenome analysis was conducted using the command `anvi-pan-genome`. The `anvi-pan-genome` command was run using the flag `"-use-ncbi-blast"` and the parameters `"-minbit 0.5"` and `"-mcl-inflation 8,"` which govern the determination of protein sequence similarity and identification of gene clusters, respectively. ANI was calculated using the command `anvi-compute-ani`, which used PyANI (80) to compute ANI across a given set of genomes. The AAI of bidirectional best-hit proteins was calculated using a Web-based calculator (81). ANI, AAI, and 16S rRNA gene heat maps were generated using the R package `gplots heatmap.2` (v 3.0.1.1) (82, 83); the dendrograms were calculated using hierarchical clustering with complete agglomeration.

Data and culture availability. Nearly full-length 16S rRNA genes of isolates FB-6 and FB-Cd derived from Sanger sequencing were deposited in GenBank under accession numbers [JN885793](#) and [JN885795](#),

respectively. The new FeOB strains were deposited in the German Collection of Microorganisms and Cell Cultures under accession numbers DSM 25805 (FB-6) and DSM 25617 (FB-Cd). The genome of strain FB-6 is available from the IMG/M database under genome ID [2523533526](https://doi.org/10.2523533526) or the NCBI database under BioProject [PRJNA178046](https://doi.org/10.1093/bioinformatics/btj178) and BioSample [SAMN02441003](https://www.ncbi.nlm.nih.gov/biosample/SAMN02441003), and the Sequence Read Archive under accession number [SRP024891](https://www.ncbi.nlm.nih.gov/sra/SRP024891). The FB-6 16S rRNA gene sequences can be found in IMG/M under the locus tags D466DRAFT_0316 and D466DRAFT_1646. The genome of strain FB-Cd is available from the IMG/M database under genome ID [2574179766](https://doi.org/10.2574179766) or the NCBI database under BioProject [PRJNA239509](https://doi.org/10.1093/bioinformatics/btj239) and BioSample [SAMN02787089](https://www.ncbi.nlm.nih.gov/biosample/SAMN02787089), and the Sequence Read Archive under accession number [SRP077360](https://www.ncbi.nlm.nih.gov/sra/SRP077360). The FB-Cd 16S rRNA gene sequences can be found in IMG under the locus tags CD04DRAFT_0503 and CD04DRAFT_3334.

SUPPLEMENTAL MATERIAL

Supplemental material is available online only.

SUPPLEMENTAL FILE 1, PDF file, 3 MB.

SUPPLEMENTAL FILE 2, XLSX file, 0.1 MB.

ACKNOWLEDGMENTS

This project was supported by the graduate research training group “Alteration and Element Mobility at the Microbe-Mineral Interface” (GRK 1257), which is part of the Jena School for Microbial Communication (JSMC), as well as by the Collaborative Research Centre 1076 AquaDiva (project no. 218627073), both funded by the German Research Foundation (Deutsche Forschungsgemeinschaft [DFG]). C.S.C. was supported by funding from National Science Foundation (NSF) Geobiology and Low Temperature Geochemistry grant EAR-1833525. J.L.K. and C.S.C. were supported by funding from ONR grant N00014-17-1-2640. M.H. was supported by a NASA Delaware Space Grant Internship, NSF EPSCoR grant no. IIA-1301765, and the State of Delaware. The work conducted by the U.S. Department of Energy Joint Genome Institute, a DOE Office of Science User Facility, is supported under contract no. DE-AC02-05CH11231. A.L. was partially supported by St. Petersburg University (ID 51555639).

We thank Gina Freyer, Andreas Fischer, Susanne Grube, Peter Bouwma, Jens Wurlitzer, Yesha Shrestha, Robert Andrews, and Cassandra Harris for technical assistance. We also thank Sandor Nietzsche for SEM imaging at the Elektronenmikroskopisches Zentrum, FSU Jena.

Any use of trade, firm, or product names is for descriptive purposes only and does not imply endorsement by the U.S. government.

We declare we have no competing financial interest.

REFERENCES

- Hallberg KB, Johnson DB. 2003. Novel acidophiles isolated from moderately acidic mine drainage waters. *Hydrometallurgy* 71:139–148. [https://doi.org/10.1016/S0304-386X\(03\)00150-6](https://doi.org/10.1016/S0304-386X(03)00150-6).
- Laroche E, Casiot C, Fernandez-Rojo L, Desoeuvre A, Tardy V, Bruneel O, Battaglia-Brunet F, Joulian C, Héry M. 2018. Dynamics of bacterial communities mediating the treatment of an As-rich acid mine drainage in a field pilot. *Front Microbiol* 9:3169. <https://doi.org/10.3389/fmicb.2018.03169>.
- Fukushi K, Sasaki M, Sato T, Yanase N, Amano H, Ikeda H. 2003. A natural attenuation of arsenic in drainage from an abandoned arsenic mine dump. *Appl Geochem* 18:1267–1278. [https://doi.org/10.1016/S0883-2927\(03\)00011-8](https://doi.org/10.1016/S0883-2927(03)00011-8).
- Hohmann C, Winkler E, Morin G, Kappler A. 2010. Anaerobic Fe(II)-oxidizing bacteria show As resistance and immobilize As during Fe(III) mineral precipitation. *Environ Sci Technol* 44:94–101. <https://doi.org/10.1021/es900708s>.
- Baker BJ, Banfield JF. 2003. Microbial communities in acid mine drainage. *FEMS Microbiol Ecol* 44:139–152. [https://doi.org/10.1016/S0168-6496\(03\)00028-X](https://doi.org/10.1016/S0168-6496(03)00028-X).
- Druschel GK, Baker BJ, Gihring TM, Banfield JF. 2004. Acid mine drainage biogeochemistry at Iron Mountain, California. *Geochem Trans* 5:13–32. <https://doi.org/10.1186/1467-4866-5-13>.
- Hallberg KB, Coupland K, Kimura S, Johnson DB. 2006. Macroscopic streamer growths in acidic, metal-rich mine waters in North Wales consist of novel and remarkably simple bacterial communities. *Appl Environ Microbiol* 72:2022–2030. <https://doi.org/10.1128/AEM.72.3.2022-2030.2006>.
- Hallberg KB, Gonzalez-Toril E, Johnson DB. 2010. *Acidithiobacillus ferrivorans*, sp. nov.; facultatively anaerobic, psychrotolerant iron-, and sulfur-oxidizing acidophiles isolated from metal mine-impacted environments. *Extremophiles* 14:9–19. <https://doi.org/10.1007/s00792-009-0282-y>.
- Lack J, Chaudhuri S, Chakraborty R, Achenbach L, Coates J. 2002. Anaerobic biooxidation of Fe(II) by *Dechlorosoma suillum*. *Microb Ecol* 43:424–431. <https://doi.org/10.1007/s00248-001-1061-1>.
- Gault AG, Cooke DR, Townsend AT, Charnock JM, Polya DA. 2005. Mechanisms of arsenic attenuation in acid mine drainage from Mount Bischoff, western Tasmania. *Sci Total Environ* 345:219–228. <https://doi.org/10.1016/j.scitotenv.2004.10.030>.
- Stumm W, Morgan JJ. 1996. *Aquatic chemistry: chemical equilibria and rates in natural waters*. John Wiley & Sons, New York, NY.
- Chen XG, Geng AL, Yan R, Gould WD, Ng YL, Liang DT. 2004. Isolation and characterization of sulphur-oxidizing *Thiomonas* sp. and its potential application in biological deodorization. *Lett Appl Microbiol* 39:495–503. <https://doi.org/10.1111/j.1472-765X.2004.01615.x>.
- Hovasse A, Bruneel O, Casiot C, Desoeuvre A, Farasin J, Hery M, Van Dorsseleer A, Carapito C, Arsène-Pløetze F. 2016. Spatio-temporal detection of the *Thiomonas* population and the *Thiomonas* arsenite oxidase involved in natural arsenite attenuation processes in the Carnoules acid mine drainage. *Front Cell Dev Biol* 4:3. <https://doi.org/10.3389/fcell.2016.00003>.

14. Battaglia-Brunet F, Joulian C, Garrido F, Dictor M-C, Morin D, Coupland K, Barrie Johnson D, Hallberg K, Baranger P. 2006. Oxidation of arsenite by *Thiomonas* strains and characterization of *Thiomonas arsenivorans* sp. nov. *Antonie Van Leeuwenhoek* 89:99–108. <https://doi.org/10.1007/s10482-005-9013-2>.
15. Duquesne K, Lieutaud A, Ratouchniak J, Muller D, Lett M-C, Bonnefoy V. 2008. Arsenite oxidation by a chemoautotrophic moderately acidophilic *Thiomonas* sp.: from the strain isolation to the gene study. *Environ Microbiol* 10:228–237. <https://doi.org/10.1111/j.1462-2920.2007.01447.x>.
16. Freil KC, Krueger MC, Farasin J, Brochier-Armanet C, Barbe V, Andrès J, Cholley P-E, Dillies M-A, Jagla B, Koechler S, Leva Y, Magdelenat G, Plewniak F, Proux C, Coppée J-Y, Bertin PN, Heipieper HJ, Arsène-Plöetze F. 2015. Adaptation in toxic environments: arsenic genomic islands in the bacterial genus *Thiomonas*. *PLoS One* 10:e0139011. <https://doi.org/10.1371/journal.pone.0139011>.
17. Casiot C, Morin G, Juillot F, Bruneel O, Personné J-C, Leblanc M, Duquesne K, Bonnefoy V, Elbaz-Poulichet F. 2003. Bacterial immobilization and oxidation of arsenic in acid mine drainage (Carnoulès creek, France). *Water Res* 37:2929–2936. [https://doi.org/10.1016/S0043-1354\(03\)00080-0](https://doi.org/10.1016/S0043-1354(03)00080-0).
18. Bruneel O, Personné J-C, Casiot C, Leblanc M, Elbaz-Poulichet F, Mahler BJ, Le Flèche A, Grimont PAD. 2003. Mediation of arsenic oxidation by *Thiomonas* sp. in acid-mine drainage (Carnoulès, France). *J Appl Microbiol* 95:492–499. <https://doi.org/10.1046/j.1365-2672.2003.02004.x>.
19. Slyemi D, Moinier D, Brochier-Armanet C, Bonnefoy V, Johnson D. 2011. Characteristics of a phylogenetically ambiguous, arsenic-oxidizing *Thiomonas* sp., *Thiomonas arsenitoxydans* strain 3As^T sp. nov. *Arch Microbiol* 193:439–449. <https://doi.org/10.1007/s00203-011-0684-y>.
20. Fabisch M, Beulig F, Akob DM, Küsel K. 2013. Surprising abundance of *Gallionella*-related iron oxidizers in creek sediments at pH 4.4 or at high heavy metal concentrations. *Front Microbiol* 4:390. <https://doi.org/10.3389/fmicb.2013.00390>.
21. Fabisch M, Freyer G, Johnson CA, Büchel G, Akob DM, Neu TR, Küsel K. 2016. Dominance of '*Gallionella capsiferiformans*' and heavy metal association with *Gallionella*-like stalks in metal-rich pH 6 mine water discharge. *Geobiology* 14:68–90. <https://doi.org/10.1111/gbi.12162>.
22. Hallenbeck M. 2019. Genomic analyses of novel iron-oxidizing *Thiomonas* isolates from acid mine drainage. Undergraduate Honors Degree thesis. University of Delaware, Newark, DE, USA.
23. Beulig F. 2010. Microbial communities involved in iron cycling at an acid mine drainage-affected creek. Master's degree thesis. Friedrich Schiller University Jena, Jena, Germany.
24. Fabisch M. 2014. Iron-oxidizing bacteria in heavy metal-contaminated creeks. PhD dissertation. Friedrich Schiller University Jena, Jena, Germany.
25. Arsène-Plöetze F, Chiboub O, Lievreumont D, Farasin J, Freil KC, Fouteau S, Barbe V. 2018. Adaptation in toxic environments: comparative genomics of loci carrying antibiotic resistance genes derived from acid mine drainage waters. *Environ Sci Pollut Res Int* 25:1470–1483. <https://doi.org/10.1007/s11356-017-0535-8>.
26. Delavat F, Lett M-C, Lièvreumont D. 2012. Novel and unexpected bacterial diversity in an arsenic-rich ecosystem revealed by culture-dependent approaches. *Biol Direct* 7:28. <https://doi.org/10.1186/1745-6150-7-28>.
27. Huber H, Stetter KO. 1990. *Thiobacillus cuprinus* sp. nov., a novel facultatively organotrophic metal-mobilizing bacterium. *Appl Environ Microbiol* 56:315–322. <https://doi.org/10.1128/AEM.56.2.315-322.1990>.
28. Lu S, Gischkat S, Reiche M, Akob DM, Hallberg KB, Küsel K. 2010. Ecophysiology of Fe-cycling bacteria in acidic sediments. *Appl Environ Microbiol* 76:8174–8183. <https://doi.org/10.1128/AEM.01931-10>.
29. Coupland K, Battaglia-Brunet F, Hallberg KB, Dictor M-C, Garrido F, Johnson DB. 2004. Oxidation of iron, sulfur and arsenic in mine waters and mine wastes: an important role for novel *Thiomonas* spp, p 639–646. In Tsezos M, Hatzikioseyan A, Remoundaki E (ed), *Biohydrometallurgy: a sustainable technology in evolution*. National Technical University of Athens, Athens, Greece.
30. Konstantinidis KT, Rosselló-Móra R, Amann R. 2017. Uncultivated microbes in need of their own taxonomy. *ISME J* 11:2399–2406. <https://doi.org/10.1038/ismej.2017.113>.
31. Battaglia-Brunet F, El Achbouni H, Quemeneur M, Hallberg KB, Kelly DP, Joulian C. 2011. Proposal that the arsenite-oxidizing organisms, *Thiomonas cuprina* and '*Thiomonas arsenivorans*' be reclassified as strains of *Thiomonas delicata*. *Int J Syst Evol Microbiol* 61:2816–2821. <https://doi.org/10.1099/ijs.0.023408-0>.
32. Lüdecke C, Reiche M, Eusterhues K, Nietzsche S, Küsel K. 2010. Acid-tolerant microaerophilic Fe(II)-oxidizing bacteria promote Fe(III)-accumulation in a fen. *Environ Microbiol* 12:2814–2825. <https://doi.org/10.1111/j.1462-2920.2010.02251.x>.
33. Shi L, Rosso KM, Zachara JM, Fredrickson JK. 2012. Mtr extracellular electron-transfer pathways in Fe(III)-reducing or Fe(II)-oxidizing bacteria: a genomic perspective. *Biochem Soc Trans* 40:1261–1267. <https://doi.org/10.1042/BST20120098>.
34. Liu J, Wang Z, Belchik SM, Edwards MJ, Liu C, Kennedy DW, Merkley ED, Lipton MS, Butt JN, Richardson DJ, Zachara JM, Fredrickson JK, Rosso KM, Shi L. 2012. Identification and characterization of MtoA: a decaheme c-type cytochrome of the neutrophilic Fe(II)-oxidizing bacterium *Sideroxydans lithotrophicus* ES-1. *Front Microbiol* 3:37. <https://doi.org/10.3389/fmicb.2012.00037>.
35. Beckwith CR, Edwards MJ, Lawes M, Shi L, Butt JN, Richardson DJ, Clarke TA. 2015. Characterization of MtoD from *Sideroxydans lithotrophicus*: a cytochrome c electron shuttle used in lithoautotrophic growth. *Front Microbiol* 6:332. <https://doi.org/10.3389/fmicb.2015.00332>.
36. He S, Barco RA, Emerson D, Roden EE. 2017. Comparative genomic analysis of neutrophilic iron(II) oxidizer genomes for candidate genes in extracellular electron transfer. *Front Microbiol* 8:1584. <https://doi.org/10.3389/fmicb.2017.01584>.
37. McAllister SM, Polson SW, Butterfield DA, Glazer BT, Sylvan JB, Chan CS. 2020. Validating the Cyc2 neutrophilic iron oxidation pathway using meta-omics of *Zetaproteobacteria* iron mats at marine hydrothermal vents. *mSystems* 5:e00553-19. <https://doi.org/10.1128/mSystems.00553-19>.
38. Amouric A, Brochier-Armanet C, Johnson DB, Bonnefoy V, Hallberg KB. 2011. Phylogenetic and genetic variation among Fe(II)-oxidizing acidithiobacilli supports the view that these comprise multiple species with different ferrous iron oxidation pathways. *Microbiology* 157:111–122. <https://doi.org/10.1099/mic.0.044537-0>.
39. Arai H, Kawakami T, Osamura T, Hirai T, Sakai Y, Ishii M. 2014. Enzymatic characterization and in vivo function of five terminal oxidases in *Pseudomonas aeruginosa*. *J Bacteriol* 196:4206–4215. <https://doi.org/10.1128/JB.02176-14>.
40. Straub KL, Benz M, Schink B. 2001. Iron metabolism in anoxic environments at near neutral pH. *FEMS Microbiol Ecol* 34:181–186. <https://doi.org/10.1111/j.1574-6941.2001.tb00768.x>.
41. Barco RA, Emerson D, Sylvan JB, Orcutt BN, Jacobson Meyers ME, Ramirez GA, Zhong JD, Edwards KJ. 2015. New insight into microbial iron oxidation as revealed by the proteomic profile of an obligate iron-oxidizing chemolithoautotroph. *Appl Environ Microbiol* 81:5927–5937. <https://doi.org/10.1128/AEM.01374-15>.
42. Kato S, Ohkuma M, Powell DH, Krepski ST, Oshima K, Hattori M, Shapiro N, Woyke T, Chan CS. 2015. Comparative genomic insights into ecophysiology of neutrophilic, microaerophilic iron oxidizing bacteria. *Front Microbiol* 6:1265. <https://doi.org/10.3389/fmicb.2015.01265>.
43. Chiu BK, Kato S, McAllister SM, Field EK, Chan CS. 2017. Novel pelagic iron-oxidizing zetaproteobacteria from the Chesapeake Bay oxic-anoxic transition zone. *Front Microbiol* 8:1280. <https://doi.org/10.3389/fmicb.2017.01280>.
44. Yarzabal A, Brasseur G, Ratouchniak J, Lund K, Lemesle-Meunier D, DeMoss JA, Bonnefoy V. 2002. The high-molecular-weight cytochrome c *Cyc2* of *Acidithiobacillus ferrooxidans* is an outer membrane protein. *J Bacteriol* 184:313–317. <https://doi.org/10.1128/jb.184.1.313-317.2002>.
45. Castelle C, Guiral M, Malarte G, Ledgham F, Leroy G, Brugna M, Giudici-Ortoni M-T. 2008. A New iron-oxidizing/O₂-reducing supercomplex spanning both inner and outer membranes, isolated from the extreme acidophile *Acidithiobacillus ferrooxidans*. *J Biol Chem* 283:25803–25811. <https://doi.org/10.1074/jbc.M802496200>.
46. Singer E, Emerson D, Webb EA, Barco RA, Kuenen JG, Nelson WC, Chan CS, Comolli LR, Ferreira S, Johnson J, Heidelberg JF, Edwards KJ. 2011. *Mariprofundus ferrooxydans* PV-1 the first genome of a marine Fe(II) oxidizing *Zetaproteobacterium*. *PLoS One* 6:e25386. <https://doi.org/10.1371/journal.pone.0025386>.
47. Emerson D, Field EK, Chertkov O, Davenport KW, Goodwin L, Munk C, Nolan M, Woyke T. 2013. Comparative genomics of freshwater Fe-oxidizing bacteria: implications for physiology, ecology, and systematics. *Front Microbiol* 4:254. <https://doi.org/10.3389/fmicb.2013.00254>.
48. Kranz RG, Richard-Fogal C, Taylor JS, Frawley ER. 2009. Cytochrome c biogenesis: mechanisms for covalent modifications and trafficking of heme and for heme-iron redox control. *Microbiol Mol Biol Rev* 73:510–528. <https://doi.org/10.1128/MMBR.00001-09>.
49. Feissner RE, Richard-Fogal CL, Frawley ER, Loughman JA, Earley KW, Kranz RG. 2006. Recombinant cytochromes c biogenesis systems I and II and

- analysis of haem delivery pathways in *Escherichia coli*. *Mol Microbiol* 60:563–577. <https://doi.org/10.1111/j.1365-2958.2006.05132.x>.
50. Badger MR, Bek EJ. 2008. Multiple RuBisCO forms in proteobacteria: their functional significance in relation to CO₂ acquisition by the CBB cycle. *J Exp Bot* 59:1525–1541. <https://doi.org/10.1093/jxb/ern297>.
 51. Chen X, Schreiber K, Appel J, Makowka A, Fähnrich B, Roettger M, Hajirezaei MR, Sönnichsen FD, Schönheit P, Martin WF, Gutekunst K. 2016. The Entner–Doudoroff pathway is an overlooked glycolytic route in cyanobacteria and plants. *Proc Natl Acad Sci U S A* 113:5441–5446. <https://doi.org/10.1073/pnas.1521916113>.
 52. Lack JG, Chaudhuri SK, Kelly SD, Kemner KM, O'Connor SM, Coates JD. 2002. Immobilization of radionuclides and heavy metals through anaerobic bio-oxidation of Fe(II). *Appl Environ Microbiol* 68:2704–2710. <https://doi.org/10.1128/aem.68.6.2704-2710.2002>.
 53. Grawunder A, Lonschinski M, Merten D, Büchel G. 2009. Distribution and bonding of residual contamination in glacial sediments at the former uranium mining leaching heap of Gessen/Thuringia, Germany. *Geochemistry* 69:5–19. <https://doi.org/10.1016/j.chemer.2008.06.001>.
 54. Merten D, Kothe E, Büchel G. 2004. Studies on microbial heavy metal retention from uranium mine drainage water with special emphasis on rare earth elements. *Mine Water Environ* 23:34–43. <https://doi.org/10.1007/s10230-004-0034-2>.
 55. Carlsson E, Büchel G. 2005. Screening of residual contamination at a former uranium heap leaching site, Thuringia, Germany. *Geochemistry* 65:75–95. <https://doi.org/10.1016/j.chemer.2005.06.007>.
 56. Man JC. 1975. The probability of most probable numbers. *Eur J Appl Microbiol* 1:67–78. <https://doi.org/10.1007/BF01880621>.
 57. Emerson D, Moyer C. 1997. Isolation and characterization of novel iron-oxidizing bacteria that grow at circumneutral pH. *Appl Environ Microbiol* 63:4784–4792. <https://doi.org/10.1128/AEM.63.12.4784-4792.1997>.
 58. Hädrich A, Cooper RE, Litzba U, Akob DM, Küsel K, Taillefert M, Wagner FE, Nietzsche S, Rösch P, Ciobota V, Popp J. 2019. Microbial Fe(II) oxidation by *Sideroxydans lithotrophicus* ES-1 in the presence of Schlöppnerbrunnen fen-derived humic acids. *FEMS Microbiol Ecol* 95:fiz034. <https://doi.org/10.1093/femsec/fiz034>.
 59. Kügler S, Cooper RE, Wegner C-E, Mohr JF, Wichard T, Küsel K. 2019. Iron-organic matter complexes accelerate microbial iron cycling in an iron-rich fen. *Sci Total Environ* 646:972–988. <https://doi.org/10.1016/j.scitotenv.2018.07.258>.
 60. Bozzola JJ. 2007. Conventional specimen preparation techniques for scanning electron microscopy of biological specimens, p 449–466. *In* Kuo J (ed), *Electron microscopy: methods and protocols*, vol 369. Humana Press, Totowa, NJ.
 61. Weisburg WG, Barns SM, Pelletier DA, Lane DJ. 1991. 16S ribosomal DNA amplification for phylogenetic study. *J Bacteriol* 173:697–703. <https://doi.org/10.1128/jb.173.2.697-703.1991>.
 62. Kearse M, Moir R, Wilson A, Stones-Havas S, Cheung M, Sturrock S, Buxton S, Cooper A, Markowitz S, Duran C, Thierer T, Ashton B, Meintjes P, Drummond A. 2012. Geneious Basic: an integrated and extendable desktop software platform for the organization and analysis of sequence data. *Bioinformatics* 28:1647–1649. <https://doi.org/10.1093/bioinformatics/bts199>.
 63. Altschul S, Gish W, Miller W, Myers E, Lipman D. 1990. Basic local alignment search tool. *J Mol Biol* 215:403–410. [https://doi.org/10.1016/S0022-2836\(05\)80360-2](https://doi.org/10.1016/S0022-2836(05)80360-2).
 64. Madden T. 2002. The BLAST sequence analysis tool. *In* McEntyre J, Ostell J (ed), *The NCBI handbook*. National Center for Biotechnology Information, Bethesda, MD, USA.
 65. NCBI Resource Coordinators. 2016. Database resources of the National Center for Biotechnology Information. *Nucleic Acids Res* 44:D7–D19. <https://doi.org/10.1093/nar/gkv1290>.
 66. DeSantis TZ, Jr, Hugenholtz P, Keller K, Brodie EL, Larsen N, Piceno YM, Phan R, Andersen GL. 2006. NAST: a multiple sequence alignment server for comparative analysis of 16S rRNA genes. *Nucleic Acids Res* 34:W394–W399. <https://doi.org/10.1093/nar/gkl244>.
 67. Ludwig W, Strunk O, Westram R, Richter L, Meier H, Yadukumar Buchner A, Lai T, Steppi S, Jobb G, Forster W, Brettske I, Gerber S, Ginhart AW, Gross O, Grumann S, Hermann S, Jost R, König A, Liss T, Lussmann R, May M, Nonhoff B, Reichel B, Strehlow R, Stamatakis A, Stuckmann N, Vilbig A, Lenke M, Ludwig T, Bode A, Schliefer K-H. 2004. ARB: a software environment for sequence data. *Nucleic Acids Res* 32:1363–1371. <https://doi.org/10.1093/nar/gkh293>.
 68. Nancucheo I, Rowe OF, Hedrich S, Johnson DB. 2016. Solid and liquid media for isolating and cultivating acidophilic and acid-tolerant sulfate-reducing bacteria. *FEMS Microbiol Lett* 363:fnw083. <https://doi.org/10.1093/femsle/fnw083>.
 69. Drake HL. 1994. Acetogenesis, acetogenic bacteria, and the acetyl-CoA “Wood/Ljungdahl” pathway: past and current perspectives, p 3–60. *In* Drake HL (ed), *Acetogenesis*. Chapman & Hall, New York, NY.
 70. Downs RT, Hall-Wallace M. 2003. The American mineralogist crystal structure database. *Am Mineral* 88:247–250.
 71. Mingkun L, Copeland A, Han J. 2011. DUK—a fast and efficient kmer based sequence matching tool. Joint Genome Institute. <https://www.osti.gov/servlets/purl/1016000>.
 72. Gnerre S, MacCallum I, Przybylski D, Ribeiro FJ, Burton JN, Walker BJ, Sharpe T, Hall G, Shea TP, Sykes S, Berlin AM, Aird D, Costello M, Daza R, Williams L, Nicol R, Gnirke A, Nusbaum C, Lander ES, Jaffe DB. 2011. High-quality draft assemblies of mammalian genomes from massively parallel sequence data. *Proc Natl Acad Sci U S A* 108:1513–1518. <https://doi.org/10.1073/pnas.1017351108>.
 73. Eid J, Fehr A, Gray J, Luong K, Lyle J, Otto G, Peluso P, Rank D, Baybayan P, Bettman B, Bibillo A, Bjornson K, Chaudhuri B, Christians F, Cicero R, Clark S, Dalal R, Dewinter A, Dixon J, Foquet M, Gaertner A, Hardenbol P, Heiner C, Hester K, Holden D, Kearns G, Kong X, Kuse R, Lacroix Y, Lin S, Lundquist P, Ma C, Marks P, Maxham M, Murphy D, Park I, Pham T, Phillips M, Roy J, Sebra R, Shen G, Sorenson J, Tomaney A, Travers K, Trulson M, Vielcieli J, Wegener J, Wu D, Yang A, Zaccarin D, Zhao P, Zhong F, Korfach J, Turner S. 2009. Real-time DNA sequencing from single polymerase molecules. *Science* 323:133–138. <https://doi.org/10.1126/science.1162986>.
 74. Chin C-S, Alexander DH, Marks P, Klammer AA, Drake J, Heiner C, Clum A, Copeland A, Huddleston J, Eichler EE, Turner SW, Korlach J. 2013. Nonhybrid, finished microbial genome assemblies from long-read SMRT sequencing data. *Nat Methods* 10:563–569. <https://doi.org/10.1038/nmeth.2474>.
 75. Eren AM, Esen ÖC, Quince C, Vineis JH, Morrison HG, Sogin ML, Delmont TO. 2015. Anvi'o: an advanced analysis and visualization platform for 'omics data. *PeerJ* 3:e1319. <https://doi.org/10.7717/peerj.1319>.
 76. Aziz RK, Bartels D, Best AA, DeJongh M, Disz T, Edwards RA, Formsma K, Gerdes S, Glass EM, Kubal M, Meyer F, Olsen GJ, Olson R, Osterman AL, Overbeek RA, McNeil LK, Paarmann D, Paczian T, Parrello B, Pusch GD, Reich C, Stevens R, Vassieva O, Vonstein V, Wilke A, Zagnitko O. 2008. The RAST server: rapid annotations using subsystems technology. *BMC Genomics* 9:75. <https://doi.org/10.1186/1471-2164-9-75>.
 77. Chen IMA, Chu K, Palaniappan K, Pillay M, Ratner A, Huang JH, Hunt-Emann M, Varghese N, White JR, Seshadri R, Smirnova T, Kirton E, Jungbluth SP, Woyke T, Eloe-Fadrosh EA, Ivanova NN, Kyrpides NC. 2019. IMG/M v.5.0: an integrated data management and comparative analysis system for microbial genomes and microbiomes. *Nucleic Acids Res* 47:D666–D677. <https://doi.org/10.1093/nar/gky901>.
 78. Stamatakis A. 2006. RAxML-VI-HPC: maximum likelihood-based phylogenetic analyses with thousands of taxa and mixed models. *Bioinformatics* 22:2688–2690. <https://doi.org/10.1093/bioinformatics/btl446>.
 79. Delmont TO, Eren AM. 2018. Linking pangenomes and metagenomes: the *Prochlorococcus* metapangenome. *PeerJ* 6:e4320. <https://doi.org/10.7717/peerj.4320>.
 80. Pritchard L, Glover RH, Humphris S, Elphinstone JG, Toth IK. 2016. Genomics and taxonomy in diagnostics for food security: soft-rotting enterobacterial plant pathogens. *Anal Methods* 8:12–24. <https://doi.org/10.1039/C5AY02550H>.
 81. Rodriguez LM, Konstantinidis KT. 2014. Bypassing cultivation to identify bacterial species, vol 9, p 111–118. American Society for Microbiology, Washington, DC. <https://doi.org/10.1128/microbe.9.111.1>.
 82. R Core Team. 2017. R: a language and environment for statistical computing, R Foundation for Statistical Computing, Vienna, Austria. <https://www.R-project.org/>.
 83. Wickham H, Chang W. 2016. ggplot2: create elegant data visualizations using the grammar of graphics. <https://cran.r-project.org/web/packages/ggplot2/>.
 84. Hallbeck L, Ståhl F, Pedersen K. 1993. Phylogeny and phenotypic characterization of the stalk-forming and iron-oxidizing bacterium *Gallionella ferruginea*. *J Gen Microbiol* 139:1531–1535. <https://doi.org/10.1099/00221287-139-7-1531>.
 85. Weiss JV, Rentz JA, Plaia T, Neubauer SC, Merrill-Floyd M, Lilburn T, Bradburne C, Megonigal JP, Emerson D. 2007. Characterization of neutrophilic Fe(II)-oxidizing bacteria isolated from the rhizosphere of wetland plants and description of *Ferritrophicum radicolica* gen. nov.

- sp. nov., and *Sideroxydans paludicola* sp. nov. *Geomicrobiol J* 24: 559–570. <https://doi.org/10.1080/01490450701670152>.
86. Emerson D, Floyd MM. 2005. Enrichment and isolation of iron-oxidizing bacteria at neutral pH. *Environ Microbiol* 397:112–123. [https://doi.org/10.1016/S0076-6879\(05\)97006-7](https://doi.org/10.1016/S0076-6879(05)97006-7).
 87. Temple KL, Colmer AR. 1951. The autotrophic oxidation of iron by a new bacterium, *Thiobacillus ferrooxidans*. *J Bacteriol* 62:605–611. <https://doi.org/10.1128/JB.62.5.605-611.1951>.
 88. Emerson D, Rentz JA, Lilburn TG, Davis RE, Aldrich H, Chan C, Moyer CL. 2007. A novel lineage of *Proteobacteria* involved in formation of marine Fe-oxidizing microbial mat communities. *PLoS One* 2:e667. <https://doi.org/10.1371/journal.pone.0000667>.
 89. Chan CS, Fakra SC, Emerson D, Fleming EJ, Edwards KJ. 2011. Lithotrophic iron-oxidizing bacteria produce organic stalks to control mineral growth: implications for biosignature formation. *ISME J* 5:717–727. <https://doi.org/10.1038/ismej.2010.173>.
 90. Battaglia-Brunet F, Dictor MC, Garrido F, Crouzet C, Morin D, Dekeyser K, Clarens M, Baranger P. 2002. An arsenic(III)-oxidizing bacterial population: selection, characterization, and performance in reactors. *J Appl Microbiol* 93:656–667. <https://doi.org/10.1046/j.1365-2672.2002.01726.x>.
 91. Bryan CG, Marchal M, Battaglia-Brunet F, Kugler V, Lemaitre-Guillier C, Lièvreumont D, Bertin PN, Arsène-Ploetze F. 2009. Carbon and arsenic metabolism in *Thiomonas* strains: differences revealed diverse adaptation processes. *BMC Microbiol* 9:127. <https://doi.org/10.1186/1471-2180-9-127>.
 92. Katayama Y, Uchino Y, Wood AP, Kelly DP. 2006. Confirmation of *Thiomonas delicata* (formerly *Thiobacillus delicatus*) as a distinct species of the genus *Thiomonas* Moreira and Amils 1997 with comments on some species currently assigned to the genus. *Int J Syst Evol Microbiol* 56:2553–2557. <https://doi.org/10.1099/ijs.0.64299-0>.
 93. Kelly DP, Uchino Y, Huber H, Amils R, Wood AP. 2007. Reassessment of the phylogenetic relationships of *Thiomonas cuprina*. *Int J Syst Evol Microbiol* 57:2720–2724. <https://doi.org/10.1099/ijs.0.65537-0>.
 94. Narayan KD, Sabat SC, Das SK. 2017. Mechanism of electron transport during thiosulfate oxidation in an obligately mixotrophic bacterium *Thiomonas bhubaneswarensis* strain S10 (DSM 18181T). *Appl Microbiol Biotechnol* 101:1239–1252. <https://doi.org/10.1007/s00253-016-7958-x>.
 95. Panda SK, Jyoti V, Bhadra B, Nayak KC, Shivaji S, Rainey FA, Das SK. 2009. *Thiomonas bhubaneswarensis* sp. nov., an obligately mixotrophic, moderately thermophilic, thiosulfate-oxidizing bacterium. *Int J Syst Evol Microbiol* 59:2171–2175. <https://doi.org/10.1099/ijs.0.007120-0>.
 96. Milde K, Sand W, Wolff W, Bock E. 1983. *Thiobacilli* of the corroded concrete walls of the Hamburg sewer system. *Microbiology* 129: 1327–1333. <https://doi.org/10.1099/00221287-129-5-1327>.
 97. Wentzien S, Sand W. 1999. Polythionate metabolism in *Thiomonas intermedia* K12, p 787–797. Elsevier, Philadelphia, PA.
 98. Wentzien S, Sand W. 2004. Tetrathionate disproportionation by *Thiomonas intermedia* K12. *Eng Life Sci* 4:25–30. <https://doi.org/10.1002/elsc.200400007>.
 99. Katayama-Fujimura Y, Kawashima I, Tszuzaki N, Kuraishi H. 1984. Physiological characteristics of the facultatively chemolithotrophic *Thiobacillus* species *Thiobacillus delicatus* nom. rev., emend., *Thiobacillus perometabolis*, and *Thiobacillus intermedius*. *Int J Syst Bacteriol* 34:139–144. <https://doi.org/10.1099/00207713-34-2-139>.
 100. London J. 1963. *Thiobacillus intermedius* nov. sp. *Archiv Mikrobiol* 46:329–337. <https://doi.org/10.1007/BF00408489>.
 101. Moreira D, Amils R. 1997. Phylogeny of *Thiobacillus cuprinus* and other mixotrophic *Thiobacilli*: proposal for *Thiomonas* gen. nov. *Int J Syst Bacteriol* 47:522–528. <https://doi.org/10.1099/00207713-47-2-522>.
 102. Farasin J, Andres J, Casiot C, Barbe V, Faerber J, Halter D, Heintz D, Koechler S, Lièvreumont D, Lugan R, Marchal M, Plewniak F, Seby F, Bertin PN, Arsène-Ploetze F. 2015. *Thiomonas* sp. CB2 is able to degrade urea and promote toxic metal precipitation in acid mine drainage waters supplemented with urea. *Front Microbiol* 6:993. <https://doi.org/10.3389/fmicb.2015.00993>.
 103. Farasin J, Koechler S, Varet H, Deschamps J, Dillies M-A, Proux C, Erhardt M, Huber A, Jagla B, Briandet R, Coppée J-Y, Arsène-Ploetze F. 2017. Comparison of biofilm formation and motility processes in arsenic-resistant *Thiomonas* spp. strains revealed divergent response to arsenite. *Microb Biotechnol* 10:789–803. <https://doi.org/10.1111/1751-7915.12556>.
 104. Arsène-Ploetze F, Koechler S, Marchal M, Coppée J-Y, Chandler M, Bonnefoy V, Brochier-Armanet C, Barakat M, Barbe V, Battaglia-Brunet F, Bruneel O, Bryan CG, Cleiss-Arnold J, Cruveiller S, Erhardt M, Heinrich-Salmeron A, Hommais F, Joulian C, Krin E, Lieutaud A, Lièvreumont D, Michel C, Muller D, Ortet P, Proux C, Siguier P, Roche D, Rouy Z, Salvignol G, Slyemi D, Talla E, Weiss S, Weissenbach J, Médigue C, Bertin PN. 2010. Structure, function, and evolution of the *Thiomonas* spp. genome. *PLoS Genet* 6:e1000859. <https://doi.org/10.1371/journal.pgen.1000859>.
 105. Duquesne K, Lieutaud A, Ratouchniak J, Yarzabal A, Bonnefoy V. 2007. Mechanisms of arsenite elimination by *Thiomonas* sp. isolated from Carnoulès acid mine drainage. *Eur J Soil Biol* 43:351–355. <https://doi.org/10.1016/j.ejsobi.2007.03.010>.
 106. Kanehisa M, Sato Y, Morishima K. 2016. BlastKOALA and GhostKOALA: KEGG tools for functional characterization of genome and metagenome sequences. *J Mol Biol* 428:726–731. <https://doi.org/10.1016/j.jmb.2015.11.006>.
 107. Reasoner DJ, Geldreich EE. 1985. A new medium for the enumeration and subculture of bacteria from potable water. *Appl Environ Microbiol* 49:1–7.